

PRINCETON UNIVERSITY OBSERVATORY
Princeton, New Jersey 08544

(NASA-CR-183222) INTERSTELLAR LINES IN THE
SPECTRUM OF SUPERNOVA 1987a Final Report,
period ending 14 Sep. 1988 (Princeton
Univ.) 60 P

N89-12510

CSCI 03A

63/89

Unclass
0162024

Final Report for NASA Grant
NAG 5-1004

Interstellar Lines in the Spectrum of Supernova 1987a

Covering the Period Ending September 14, 1988

Submitted to:

GODDARD SPACE FLIGHT CENTER
NATIONAL AERONAUTICS AND SPACE ADMINISTRATION
Greenbelt, MD 20771

By: Edward B. Jenkins
Edward B. Jenkins
Principal Investigator
Princeton University Observatory
Princeton, N. J. 08544
Tel: 609-452-3826

Co-Investigator:
Charles L. Joseph, Princeton University

October 3, 1988

1. BACKGROUND

Shortly after Supernova 1987a exploded, IUE recorded on the U. S. and European shifts several high resolution spectra before the object's ultraviolet flux had faded. Within a day or two, we and a number of other groups applied to the observatory director, Dr. Yoji Kondo, to obtain permission to analyze the spectra. That permission was granted to us, and on July 24, 1987 Princeton submitted a proposal to GSFC to obtain funding which would support our investigation.

Our primary interest was to analyze the interstellar lines produced by gases along the line of sight which reside in our galactic plane and halo, as well as material in the LMC or the immediate environment of the supernova. Initially, our motive was to generate a brief paper within a short time scale, giving a cursory treatise on the properties of the absorption lines and a first-order interpretation of the implications. It soon became apparent that others, notably the Harvard/GSFC collaboration and a group of scientists affiliated with ESA, had similar intentions and already had a head start on us. We therefore reformulated our approach and elected to embark on a longer range effort to analyze the results at a higher level of sophistication. We, Dr. Blair Savage (U. Wisconsin) and Dr. Klaas de Boer (U. Bonn, FRG) then agreed to collaborate on many of the phases of the proposed research.

One might have asked, "Why is it important to understand the lines toward the supernova, when similar information is available to us from the other stars in the LMC?" The answer is that the quality of the profiles displayed by the supernova was far superior to that obtained from the 11th, 12th and 13th magnitude stars. The exposure levels in one of the two supernova spectra was excellent, and the duration of the exposure was so short that there was negligible particle background fogging. For the O and B type stars in the LMC, the fluxes are so weak that exposures must run for many hours, and even then, the intensity levels are less than optimum. A further advantage in using the supernova spectrum for interstellar line analysis was that the continuum was perfectly smooth. For stars, there are usually interfering stellar lines to add confusion.

2. RESEARCH EFFORT COVERED BY THE GRANT

First, we attempted to forecast the probable approaches of the other approved investigators, so that we could avoid duplicating their research programs as much as possible. It was for this reason that we did not embark upon a standard abundance analysis of the gases, but instead concentrated on an interpretation of the ionization and fine-structure excitation of assorted atoms. Our goal here was to learn more about conditions in various regions of space and perhaps identify the probable origins for some velocity components whose locations were uncertain.

Shortly after the grant was in effect, B. Savage obtained data on tapes for all of the high resolution spectra recorded for the supernova. Since the proprietary period had expired, he could gain access to the European data in addition to the US exposures he was entitled to under the terms of the discretionary time ruling by the observatory director.

In the year following the data acquisition, we analyzed the results and created some interpretations which we believe to be unique. At the end of the grant period, we finished writing the scientific paper and submitted it for publication to the *Astrophysical Journal*. We have yet to receive the referee's comments. A copy of the paper in its present form is included as an addendum to this report. There is some likelihood that the paper will be modified after we obtain the referee's report. We anticipate that it will appear in the journal in about a year from now.

We have no plans to carry out additional research on the IUE spectrum of supernova 1987a.

Addendum to Final Report for NASA Grant
NAG 5-1004

Paper submitted to the Astrophysical Journal

UV OBSERVATIONS OF INTERSTELLAR ABSORPTION LINES TOWARD SN1987A

Blair D. Savage^{1,2}

Edward B. Jenkins^{1,3}

Charles L. Joseph^{1,3}

Klaas S. de Boer^{1,4}

¹ Guest Observers with the International Ultraviolet Explorer satellite, sponsored and operated by the National Aeronautics and Space Administration (USA), by the Science and Engineering Research Council (UK), and by the European Space Agency.

² Washburn Observatory, University of Wisconsin-Madison, USA

³ Princeton University Observatory, USA

⁴ Sternwarte, University of Bonn, Bonn, F.R. Germany

ABSTRACT

An average of all high resolution UV spectra of supernova 1987A recorded by IUE a few days after the explosion reveals numerous interstellar absorption lines between 1200 and 3100 Å. Features produced in the neutral medium of our galaxy and the LMC (e.g. those arising from O I, C I, C II, Mg I, Mg II, Fe II, Mn II, Si II, Ni II, etc.), together with lines from much higher stages of ionization (Al III, Si IV and C IV), were recorded with far greater fidelity than for previous observations toward stars in the LMC, owing to the supernova's extraordinary brightness and very smooth continuum.

Although profiles are shown for a large number of species, our study emphasizes the absorption produced by the more highly ionized species including Al III, Si IV and C IV. The observed absorption line velocity structure which covers the heliocentric velocity range from -30 to 330 km s⁻¹ is very complex. In our discussions, we assume that the absorption with $v < 120$ km s⁻¹ occurs in the Milky Way and its halo while the absorption with $v > 190$ km s⁻¹ occurs in the LMC. The line profiles for Al III, Si IV and C IV are converted into plots of optical depth (and column density) versus velocity. In the velocity range which we believe pertains to the Milky Way, we find that the profiles for Si IV and C IV are quite similar and much smoother than the jagged appearing Al III profile. On relating column densities, we find that while the C IV to Si IV ratio is relatively constant (ranging from 3 to 5) over the velocity range from 0 to 100 km s⁻¹, the C IV to Al III and Si IV to Al III ratios vary by nearly a factor of 10. This suggests that the C IV and Si IV along this sight line in the Milky Way and its halo may have a common origin which differs from that for Al III. Al III is almost certainly produced by ultraviolet photoionization in the gas of the Milky Way disk and low halo. A different origin is therefore suggested for Si IV and C IV.

Absorption lines created by gas in the immediate surroundings of the supernova are hard to differentiate from the very strong features created by foreground, more generally distributed material in the LMC. The best line for highlighting gas very near the supernova, the 1264 Å line from Si II in an excited fine-structure level, indicated that out to about 10 pc from the supernova the density of a mass-loss wind from the progenitor in its red giant phase is consistent with a total flux divided by the wind velocity $\dot{M}/v_w < 1 \times 10^{-6} M_{\odot} \text{ yr}^{-1} (\text{km s}^{-1})^{-1}$. With the small accumulation of gas from such a wind, it does not appear possible that the pulse of energetic photons created during the supernova's shock breakout could explain the strong Si IV and C IV features at LMC velocities.

I. INTRODUCTION

The occurrence of the brightest supernova in 384 years (SN 1987A) has provided a unique opportunity for the study of interstellar gas between the Sun and the Large Magellanic Cloud (LMC). The 50 kpc sight line to the LMC samples interstellar matter which includes dense Milky Way disk gas, low density Milky Way halo gas, low density LMC halo gas, dense LMC disk gas and gas in the circumstellar environment of the supernova itself. The favorable radial velocity of the LMC of about 280 km s^{-1} Doppler shifts absorption features associated with the LMC away from those belonging to the Milky Way. For a relatively short period after its discovery, SN 1987A was very bright in the far- and middle-ultraviolet wavelengths accessible to the spectrographs aboard the International Ultraviolet Explorer (IUE) Satellite. Through the efforts of the staff at the US and European IUE control stations, the high dispersion spectra listed in Table 1 were obtained. The preliminary analysis of these data (de Boer et al. 1987; Dupree et al. 1987) has confirmed the exceedingly rich character of the interstellar medium between the sun and the LMC which was established through earlier IUE observations of bright LMC stars by Savage and de Boer (1979, 1981). An atlas of IUE interstellar line profiles for the sight line to SN1987A based on the European data is found in Blades et al. (1988).

The optical interstellar absorption line data now available for SN 1987A are among the best available for any interstellar line of sight and reveal the wealth of information which potentially resides in such data (Vidal-Majar et al. 1987; Magain 1987; Pettini et al. 1988). While the IUE spectra have only moderate photometric quality and substantially lower resolution than most observations from the ground, a principal advantage of the UV coverage is that it includes a very wide range of ionization and encompasses a large number of the more abundant elements. The supernova is a particularly good background source, since it provides a relatively smooth background continuum against which narrow and sometimes broad interstellar lines can be viewed. As a result, uncertainties in measuring interstellar lines attributable to continuum placement will be much smaller for large sections in the supernova spectra than for typical measures of absorption toward LMC stars by Savage and de Boer (1981) or in the more recent work of Savage and Meade (1989).

In this paper we have averaged the spectra listed in Table 1 in order to obtain UV absorption line profiles of the highest possible quality in the direction of SN1987A. All of these spectra were

recorded before the supernova had faded to the point where contributions from the adjacent early type stars became important (Blades et al. 1988). The details of the averaging process and plots of the resultant profiles are found in §II. The analysis discussed in §III and §IV is mostly concerned with the new information provided by these data about the origin of the interstellar absorption lines produced by C IV, Si IV and Al III at both Milky Way and LMC velocities.

Through the analysis of an absorption line which is unlikely to have strong contributions from foreground material in the LMC, our observations can place an upper limit on the amount of circumstellar ejecta from the supernova's progenitor. This limit, in turn, indicates that very little of the strong Si IV and C IV absorption is created by a flash photoionization of nearby material at the time of the supernova's shock breakout.

II. OBSERVATIONS AND REDUCTIONS

The interstellar absorption line observations presented here were obtained with the two echelle spectrographs aboard the IUE satellite. The spectrographs, their respective SEC detectors and UV to visual light converters cover the far-UV (1150 to 2000 Å, SWP camera) and middle-UV (1800-3300 Å, LWP camera) regions of the spectrum with spectral resolutions of approximately 20 to 25 km s⁻¹ (FWHM). For details of the IUE satellite and its spectrographs see Boggess et al. (1978a,b). The individual spectra were processed at the Goddard Space Flight Center or at the ESA IUE analysis facility in the standard way with version 2 of the IUE software (Turnrose and Thompson 1984).

Table 1 lists the spectra for which multiple high dispersion IUE spectra have been averaged in order to obtain interstellar line profiles with higher signal to noise than is available in single spectra. The various spectra were all obtained with the supernova centered in the large (10"x20") entrance aperture. As a result, the alignment of true spectroscopic features with respect to detector fixed pattern noise structure will be approximately the same for all the exposures with a given detector. Therefore, the averaging process will not appreciably reduce the effects of detector fixed pattern noise. Table 1 lists the exposure time and the date and time of the observations which were obtained at both the NASA and ESA ground stations. The supernova faded very rapidly during its early evolution particularly at far-UV wavelengths. Therefore, the various spectra differ in quality and in wavelength coverage. The comments to Table 1 indicate spectral regions with weak signal levels and also spectral regions with detector saturation problems. In producing average spectra we have rejected data in saturated spectral regions and in spectral regions with very low signal levels. Most of the final profiles were determined by averaging the data from more than two images as indicated in the column of Table 1 that lists the wavelength regions of the various spectra which were used in the averaging.

The various spectra were averaged by first establishing the velocity shift required to bring the spectra into a common velocity system. This was done with reference to the many interstellar lines seen in the spectra. The zero point of the velocity scale was taken to be that provided by images SWP 30379, 30381 and 30383 at $\lambda < 1800 \text{ \AA}$. The velocity shifts of the long wavelength data were obtained by making the middle UV lines of Fe II have the same velocity as the Fe II $\lambda 1608.456 \text{ \AA}$ line. The velocity shifts actually applied to the individual spectra are listed in Table 1. Velocity

shifts of up to -18 km s^{-1} were required to register the LWP images to the average of SWP 30379, 30381 and 30383. Within a single image there was no attempt to allow for different velocity shifts from line to line with the exception of the lines of Si II $\lambda 1808$ and Al III $\lambda\lambda 1854$ and 1862 . Because of detector saturation, the data for these lines were obtained from a number of images which had weak signals for $\lambda < 1800 \text{ \AA}$. The registration of the data for these lines was to the scale established by SWP 30379. We note through our efforts to bring these data into velocity registration that 2σ velocity uncertainties of about 8 km s^{-1} exist in the combined data. Differences this large occasionally exist between our presentation of the results and the atlas of Blades et al. (1988) which are based on the European data alone and for which no special corrections were applied.

In the averaging process the measured signal (i.e. flux x integration time) for the individual spectra are linearly interpolated into 5 km s^{-1} velocity bins and added. The wavelength uncertainties introduced by the averaging process degrades the spectral resolution of the final data. We estimate that the resolution of the averaged data is approximately 25 km s^{-1} (FWHM).

For selected lines of particular interest (e.g. Si II* $\lambda 1264.730 \text{ \AA}$) where even the averaged data are very noisy, we have smoothed the averaged spectra by applying a triangular weighting function to three adjacent 5 km s^{-1} velocity bins with a weighting function of 0.5, 1.0 and 0.5.

In the processing of the individual spectra, the linearized data numbers extracted from the image were corrected for the instrumental background, the echelle blaze function and the instrumental sensitivity using the standard procedures described in Turnrose and Thompson (1984). For absorption lines with $\lambda < 1300 \text{ \AA}$ for the SWP spectra and for $\lambda < 2300 \text{ \AA}$ with the LWR spectra, where the crowding of echelle orders causes this procedure to over estimate the appropriate background, an additional level shift was determined with reference to the cores of the very strong interstellar lines in these wavelength regions. This additional shift typically amounted to 10 to 20 percent of the continuum level.

The velocity structure of the interstellar absorption to the LMC is exceedingly complex and not easily summarized with words or tables. We have therefore provided plots of the average observed flux from the supernova in the vicinity of many of the interesting interstellar lines which are within the detection capabilities of the IUE. The lines plotted and echelle orders from which the data are obtained are listed in Table 2. In some cases, more than one absorbing species produces a line in

each short region of the spectrum plotted as indicated in Table 2 . The line profile plots on a heliocentric velocity scale are shown in Figure 1 . For the direction of the supernova, one should subtract 16 km s^{-1} from a heliocentric velocity to obtain the velocity in the local standard of rest. Detector reseaux are identified on the profile plots with the letter R.

III. RESULTS

The UV interstellar absorption line spectrum seen toward SN 1987A contains information about a large number of phases of the interstellar medium in both the Milky Way and in the LMC. These phases include those producing such neutral gas features as O I, C I, Mg I, and Cl I to the highly ionized gas absorption phases responsible for the lines of Al III, Si IV, C IV and N V. In addition, the absorption features of C II, Si II and Mg II with their large f values are sensitive to intervening gas having extremely low column densities. The emphasis in this paper is on the properties and origin of the absorption features produced by the most highly ionized gas found at both Milky Way and LMC velocities.

a) Velocities

The complex structure exhibited in Figure 1 appears to be a general characteristic of the LMC sight line, which passes through a large number of different absorbing regions in the Milky Way and in the LMC (de Boer and Savage 1980 ; Savage and de Boer 1981; Songaila et al. 1986).

Vidal-Madjar et al.(1987) noted in their very high signal to noise and high resolution (FWHM = 3 km s⁻¹) spectra the presence of possibly 23 distinct absorption components in the heliocentric velocity range of 0 to 300 km s⁻¹. Some of these many components may represent sub-structure within main components.

The principal components seen in the IUE data for low ionization species occur at heliocentric velocities of approximately 15, 65, 120, 170, 220 and 280 km s⁻¹. These velocities actually refer to features which are blends of components, a result which is apparent with reference to the higher resolution Ca II line data. For example the 15 km s⁻¹ component seen in the IUE data for low ionization species such as Si II, Mg I, and Fe II is actually probably composed of components near 9, 16 and 23 km s⁻¹ while the 65 km s⁻¹ feature is probably composed of absorption components near 40, 57, 65, 72, and 75 km s⁻¹ and the very strong feature near 280 km s⁻¹ probably contains seven subcomponents spread over the velocity range 250 to 295 km s⁻¹ with the strongest components near 280 and 286 km s⁻¹ (Vidal-Madjar et al. 1987). The velocities inferred from the IUE data exhibit differences from one ion to the next. Some of these differences undoubtedly are produced by ion to ion differences in the relative strengths of the many components created by differences in the excitation conditions, elemental abundances (and their gas phase depletions), and perhaps the degree of line saturation.

The low ionization lines which have large f values, such as those of C II, Mg II and Si II, are extremely strong and wide. For example, the Mg II λ 2795.528 line exhibits nearly total absorption between -10 and +300 km s⁻¹ and has half intensity absorption velocities, v_- and v_+ , which range from -30 to +330 km s⁻¹. It is apparent from these strong lines that there exist low ionization components of absorption near approximately -15 and +315 km s⁻¹ which are not seen in Ca II absorption.

The higher ionization lines of Al III, Si IV and C IV exhibit absorption with components having their peak absorption centered near heliocentric velocities of 20, 65, 200 and 280 km s⁻¹. The very strong feature centered near 280 km s⁻¹ is certainly multicomponent in character with two or more components absorbing in the range from 250 to 300 km s⁻¹ being required to explain the breadth and shape of the feature. While weaker absorption occurs at other velocities, its component structure is not well enough defined to make velocity assignments possible. In the velocity range from -50 to +200 km s⁻¹, the high ionization C IV lines have a distinctly "smoother" appearance than do the lines of Al III and Si IV or the lines of species in lower ionization states having roughly similar absorption line depths (e.g. Si II λ 1808.00, Mg I λ 2852.127, Fe II λ 1608.456). A more quantitative comparison of the similarities and differences between the absorption profiles for the highly ionized species and some of the lower ionization species is found in §IIIb.

The IUE data in the region of the N V doublet at $\lambda\lambda$ 1238.821 and 1242.804 are extremely noisy. Useful information on the presence or absence of interstellar N V can only be obtained by processing the individual IUE echelle orders containing the lines of the N V doublet with a spectral extraction routine that properly corrects for the detector fixed pattern noise. Until this work is done, we consider any statements in the literature about the presence or absence of interstellar N V absorption toward the supernova based on the spectra we have examined as quite tentative.

b) Profile Analysis Technique

In a conventional analysis of interstellar absorption lines, one identifies specific velocity components, measures their equivalent widths, and then derives column densities using a curve of growth based on the saturation behavior of a simple Gaussian distribution of radial velocities. However, for the features seen in the supernova spectrum, the principal, seemingly distinct components are sometimes blended together by the instrumental profile. Also, as we pointed out earlier we know from high resolution recordings of the absorption features from K I, Na I and Ca II

in the supernova spectrum at visible wavelengths that single peaks in the IUE spectra are actually composed of complex, narrower components.

One might be tempted to try to use the high resolution data to create a detailed model that reconstructs how the ultraviolet lines should saturate as they grow stronger. Except in special circumstances, this is a hazardous undertaking for several reasons. First, different atomic species exhibit different patterns of absorption. The Ca II lines toward the supernova are more numerous and somewhat less "spiky" than the Na I or K I lines. This is probably a consequence of drastic reductions in the calcium depletion for components which have been shocked and accelerated -- a phenomenon recognized long ago for material within the galactic plane (Routly and Spitzer 1952). Second, the fractions of atoms existing in stages of ionization below those favored for H I regions scale with the local electron densities (and inversely with the density of ionizing radiation). Because the interstellar medium is heterogeneous, the curves of growth of such lines can differ from those of atoms in their favored (and higher) ionization stages (Spitzer and Jenkins 1975). Finally, an even cursory examination of the IUE data for ions with differing excitation potentials provide direct evidence that no single velocity pattern is globally appropriate.

For the reasons given above, we chose to present and interpret the IUE data in the following, graphical fashion. After defining a continuum level $I_c(\lambda)$, we converted residual intensities $I(\lambda)$ into *apparent* optical depths according to the relation

$$\tau(\lambda) = \ln[I_c(\lambda)/I(\lambda)] . \quad (1)$$

It is important to note, however, that the $\tau(\lambda)$ defined above correctly depicts a smoothed optical depth *only* under the conditions that $\tau(\lambda) \ll 1$ or else the velocity structure is fully resolved by the instrument.

As a start, we shall examine the behavior of the velocity structure exhibited by an ion which is expected to be abundant in ordinary H I and H II regions. Figure 2 shows logarithmic plots of the apparent τ 's of the column density based on the three absorption lines of Si II. In the plot, the curves for different lines are displaced vertically on the logarithmic scale so that each would depict the logarithm of a column density per unit velocity

$$\log [N(v)] = \log \tau - \log f \lambda + 14.576 [\text{cm}^{-2} (\text{km s}^{-1})], \quad (2)$$

if the τ 's were indeed valid. The f values for the transitions are those given by Shull, Snow and York (1981). The fact that the curves for the strong lines at 1304 and 1526Å are significantly below that of

the weaker line at 1808 Å indicates that unresolved, saturated profile structures are present.

As an experiment, we simulated how the τ plots would behave if IUE were observing absorption lines of different strength from an element whose detailed velocity profiles were identical to those of Ca II. To do this, we generated a family of $\log \tau$ plots by raising the Ca II absorption line residual intensities to various powers, smoothing them by the IUE instrumental profile¹, and then performing the conversions according to equations 1 and 2. Except for some overall changes in abundance from one velocity complex to another, the relative vertical positions of the simulated profiles agreed with those shown in Fig. 2 for identical differences in $\log f\lambda$. This concordance indicates that the generally complex and ragged character of the Ca II velocity profiles is duplicated by Si II. If we accept the Ca II profile structures as a valid model for those of Si II, we also learn from our simulation that for $v < 220 \text{ km s}^{-1}$ the $\log(\tau)$ depicted by the weak 1808 Å line is a valid representation for the true $\log(N/f\lambda)$ (i.e., it is not just a lower limit).

The shoulder located at -40 km s^{-1} in the 1808 Å line seems to have no counterpart in the 1304 or 1526 Å lines. While there is a strong transition of S I at 1807.311 Å, its apparent velocity with respect to the Si II line should be -116 km s^{-1} . A strong absorption by neutral atoms at about $+75 \text{ km s}^{-1}$ is not indicated by the high resolution data for K I or Na I (Vidal-Madjar et al. 1987).

c) Interpretation of Al III, Si IV and C IV Profiles

We now focus on the profile shapes in the IUE recordings of absorption features ascribed to highly ionized species. Figures 3 to 5 show the optical depth plots for Al III, Si IV and C IV, respectively. For each ion, the transition probability of one line is twice that of the other. After moving $\log \tau$ of the weak Al III 1862.795 Å line up by 0.3, in order to compensate for differences in $\log(f\lambda)$, we find the curve agrees well with that of the stronger 1854.720 Å line for the velocity component we identify with the LMC, while the right-hand peak in the group we identify with our galaxy (at 65 km s^{-1}) exhibits a small disagreement. As with Si II, the magnitudes of the differences between the strong and the weak lines are generally consistent with what we have constructed from

¹ The IUE instrumental profile at high resolution has a measured FWHM of approximately 20 km s^{-1} for $1300 < \lambda < 1600 \text{ Å}$ and 26 km s^{-1} for $\lambda \sim 1800 \text{ Å}$ (Evans and Imhoff 1985). In our reconstruction of the profiles, we assumed a Gaussian functional form with these widths and then calculated the modification caused by the additional smoothing and binning in our data reduction.

the high resolution data for Ca II. These differences are smaller than those seen in Figure 2 because the actual optical depths are considerably less.

Between -20 and 100 km s^{-1} , the prominent, double-peaked structure seen for Si II and Al III is not nearly as well defined in Si IV, and it is weaker yet in C IV. Furthermore, there is no disparity in the inferred $\log N(v)$ between the strong and weak lines for Si IV or C IV, even though the lines are strong. These results indicate that the velocity structure of the more highly ionized species is somewhat smoother than for the lower excitation ions.

Since the two tracings in Figures 3, 4 and 5 for the strong and weak lines of Al III, Si IV and C IV generally agree with each other, we can be confident that a simple integration of optical depths over velocity should yield column densities which are free of appreciable systematic errors caused by the smoothing of unresolved, saturated structures. Table 3 lists logarithms of the column densities obtained in this manner over three velocity intervals: (1) $v < 120 \text{ km s}^{-1}$, (2) $120 < v < 190 \text{ km s}^{-1}$ and (3) $v > 190 \text{ km s}^{-1}$. The lower and upper limits ("l.l." and "u.l.", respectively) refer to excursions in the values which would be permitted by systematic errors in the placement of the continuum level and/or the assumed background (zero) intensity. In effect, these column densities represent integrations along profiles connecting the lower or upper sets of small circles in the figures. Errors in the continuum level were assumed to be equal to the observed rms deviations of intensity about the continuum, divided by $(p/3)^{1/2}$ where p is the number of intensity points used to define the height and shape of the continuum. (The factor 3 is our estimate for the coherence length of the errors.) We estimated that the 1σ error in the background corresponded to about 5% of the local continuum level. The limits in the table do not include additional errors caused by random noise for individual intensities within the profiles. Over the velocity intervals where the absorption features are relatively strong (intervals 1 and 3), these errors are less important than the systematic errors from the background and continuum placements. For Si IV and C IV within the interval 3, the lines are so saturated in the middle that we can only estimate lower limits for $\log(N)$.

Another way of considering the similarities and differences between the profiles for Al III, Si IV and C IV is to view the column density ratios as a function of velocity between these species. Plots of $N(\text{Si IV})/N(\text{Al III})$, $N(\text{C IV})/N(\text{Al III})$ and $N(\text{C IV})/N(\text{Si IV})$ as a function of velocity are shown in Figures 6, 7 and 8. While the comparisons of Si IV and C IV with Al III exhibit large variations, it is interesting how the ratio of Si IV to C IV is relatively constant with velocity.

IV. DISCUSSION

Our discussion of the interstellar absorption line data toward SN 1987A will be divided into four sections. Section IVa will consider the possible physical location of the gas which produces the various absorption components found in the SN interstellar line spectrum. Section IVb will concern absorption which we believe is likely occurring in the Milky Way and its gaseous halo. Section IVc discusses LMC gas, and §IVd discusses the circumstellar environment of the SN. The emphasis in these discussions will be on the results relating to the most highly ionized species accessible to the IUE (e.g. Al III, Si IV and C IV). However, in the case of the SN circumstellar environment we also consider the excited fine structure levels of Si II.

a) Physical Location of the Absorbing Gas

Because of the kinematical complexity of the observed absorption spectrum toward the LMC, it is difficult to unambiguously determine the physical location of the gas producing the various absorption components detected in the IUE data. It is certainly reasonable to assign components near v_{Helio} of about 15 km s^{-1} which corresponds to v_{LSR} of -1 km s^{-1} to absorption by relatively local Milky Way gas and the components near the LMC radial velocity of about 280 km s^{-1} with absorption by gas in the LMC. The uncertainty concerns the components having the intermediate heliocentric velocities of approximately $65, 120, 170, 200, 220 \text{ km s}^{-1}$. In their studies of six stars in the direction of the LMC, Savage and de Boer (1979, 1981) and de Boer and Savage (1980), found that most LMC sight lines have absorption components near 65 and 120 km s^{-1} and additional components at velocities greater than about 160 km s^{-1} . Savage and de Boer (1981) attributed the components near 65 and 120 km s^{-1} to absorption by distant Milky Way halo gas and believed the higher velocity components were more likely associated with the LMC and its halo. Songiala et al. 1986 have proposed instead that the intermediate velocity components are more likely associated with the LMC and that the LMC sight line has an anomalously large number of absorption components which might arise from the dynamical interaction between the Milky Way and LMC. While the supernova data generally confirm the complex absorption characteristics of the LMC sight line, the data do not help particularly in resolving the the controversy which surrounds the assignment of the physical location of the absorbing components.

In order to organize the following discussions which emphasize the absorption in Al III, Si IV and C IV, we will assume that the features near 15 and 65 km s^{-1} are associated with the Milky

Way and that the components with $v > 190 \text{ km s}^{-1}$ most likely arise in the LMC. We will not discuss the likely site of origin for the weak high ionization absorption occurring between 120 and 190 km s^{-1} .

b) Milky Way Gas

The line profiles for C IV, Si IV and Al III toward the SN in the velocity range $v < 120 \text{ km s}^{-1}$ provide important new clues about the highly ionized gas in the Milky Way disk and halo. These data are of higher quality than the existing measurements for the LMC or SMC sight-lines and can be more reliably analyzed because of the relatively smooth continuum produced by the supernova. Our comments about these new data will draw heavily on the extensive amount of past work undertaken with the IUE to probe the characteristics of the highly ionized gas in the Milky Way disk and halo (for recent reviews see Savage 1987,1988; and Jenkins 1987).

The first detection of highly ionized gas in the Milky Way halo was for the sight line to R144 in the LMC (Savage and de Boer 1979). Subsequent observation of other LMC and SMC stars with the IUE revealed the pervasive nature of that gas (Savage and de Boer 1981). The sight line to the LMC passes in a direction ($l \approx 280^\circ$, $b \approx -33^\circ$) for which differential galactic rotation will produce positive velocity shifts in the position of absorption lines. In fact the positive velocity extensions to about 100 km s^{-1} of the early LMC interstellar absorption line data were rotationally analyzed to infer that the density distributions of Si IV and C IV away from the galactic plane were approximately represented by an exponential distribution with a scale height of about 4 kpc (Savage and de Boer 1981). The rotational analysis assumed the co-rotation of gas in the halo with gas in the underlying disk. However, subsequent studies of the motions of halo gas have revealed that gas at large distances from the galactic plane probably rotates more slowly than gas in the underlying disk (de Boer and Savage 1983; Kaelble, de Boer and Grewing 1985). Allowing for this effect would reduce the scale height estimate of 4 kpc.

A more reliable way of determining the distribution of highly ionized gas with distance away from the galactic plane is to produce plots of $\log [N(\text{ion})|\sin b|]$ versus $\log |z|$ for stars at a wide range of $|z|$ distances (Pettini and West 1982; Savage and Massa 1987). These plots reveal that the Si IV and C IV density distributions are very patchy with a peak to peak spread of about 1 dex. The average behavior of $\log [N(\text{ion})|\sin b|]$ versus $\log |z|$ suggests that the density stratification is roughly consistent with an exponential density distribution having a scale height of about 3 kpc

combined with a sudden density enhancement near $|z|$ of about 1 kpc which produces a sudden increase in $N(\text{ion})|\sin b|$ of about a factor of 2 to 3.

Theories for the origin this highly ionized gas in the galactic halo must be able to explain the support of the gas and ionization of the gas. Two competing models for the support of the gas are the "galactic fountain model" (Shapiro and Field 1976; Bregman 1980) and the cosmic ray supported halo models (Hartquist, Pettini and Tallant 1984; Chevalier and Fransson 1984). In the galactic fountain model, gas will be propelled into the halo as a consequence of supernova explosions which heat and elevate the pressure of gaseous regions in the galactic disk. The regions of elevated pressure may break out from the galactic plane and provide an injection of gas into the halo where the gas may cool and return to the disk in a flow pattern resembling a fountain. A process that will occur on a more gradual basis is "galactic convection". Here it is recognized from far ultraviolet absorption line studies of O VI (Jenkins 1978) and diffuse soft X-ray studies (McCammon et al. 1983) that there exists in the galactic disk a hot ($T \approx 0.3$ to 2×10^6 K), low density ($n \approx 10^{-3} \text{ cm}^{-3}$) phase of the interstellar medium which may fill much of the volume of the galactic disk. Hot (10^6 K) gas in the solar region of the galaxy is buoyant. Its thermal scale height is about 7 kpc. The gas will therefore tend to flow outward away from the galactic plane into the halo where it may cool and return to the disk as cooler clouds in a convective exchange.

In the cosmic ray supported halo models, the gas is supported at its large z by the pressure of outwardly streaming cosmic rays. Here, instead of collisional ionization by electrons at a temperature of 0.8 to 2×10^5 K, the high state of ionization may be created by energetic photons from hot white dwarf stars (Dupree and Raymond 1983), normal population I stars or from the extragalactic EUV background. A number of recent calculations have concentrated on determining the production of the highly ionized gas by photoionization (Hartquist, Pettini and Tallant 1984; Chevalier and Fransson 1984; Fransson and Chevalier 1985; Bregman and Harrington 1986). From this work it appears possible to understand the observed amounts of Si IV and C IV and in particular the sudden rise in $N(\text{ion})|\sin b|$ near $z = 1$ kpc from photoionization by the EUV background. However, the various calculations have difficulty producing the amount of N V observed toward halo stars (Savage and Massa 1987). N V is an important ion since among those ions accessible to the IUE, it requires the greatest amount of energy for its production (77 eV). Most hot stars containing He have strong He^+ edges at 54 eV. Therefore, the only stellar sources

that might be capable of converting N IV into N V are the very hot hydrogen white dwarfs.

In Table 4 we list the column density results, $N(\text{ion})|\sin b|$, obtained for Milky Way halo stars (Savage and Massa 1987), for HD 5980 in the SMC (Fitzpatrick and Savage 1983), for HD 36402 in the LMC (Savage and de Boer 1981) and for SN 1987A (this paper, see Table 3). We note that the new SN results for Al III, Si IV and C IV are very similar to the values previously obtained toward HD 36402 in the LMC. The factor of 3 difference between $N(\text{ion})|\sin b|$ toward the LMC and SMC may be simply the result of the patchy nature of the high ionization absorption in the halo.

A galactic fountain flow provides an explanation for some of the high ionization gas seen in the galactic halo in absorption and emission. Edgar and Chevalier (1986) have calculated the amount of Si IV, C IV, N V and O VI produced in cooling gas in a galactic fountain flow. For a fountain mass flow rate of four solar masses a year on each side of the galactic plane, they predict the column densities perpendicular to the galactic plane listed in Table 4. With a mass flow rate 2 times higher, their cooling gas calculation also predicts C IV and O III] *emission* line strengths which are compatible with the diffuse UV background measurements of Martin and Bowyer (1987). Thus the combination of N V absorption and C IV emission gives strong support for the presence of hot cooling gas in the galactic halo.

Although the cooling gas calculations of Edgar and Chevalier (1986) are able to produce enough N V and C IV to be consistent with the IUE measurements of halo stars and extragalactic sources, the amount of Si IV expected in the cooling gas is about three to five times smaller than observed. Because of this problem and the sudden observed increase in $N(\text{ion})|\sin b|$ near 1 kpc, it appears that a complete explanation for the presence of Si IV, C IV and N V in the halo may require the operation of a galactic fountain in the presence of ionizing galactic and extragalactic radiation. In this more complicated situation most of the observed N V would be produced in collisionally ionized cooling fountain gas while most of the observed Si IV would be produced by photoionization of high $|z|$ gas. The C IV would represent an intermediate situation with important contributions coming from cooling fountain gas and from photoionization. If this description is correct, one might expect to record differences in the appearances of absorption line profiles for species primarily produced by photoionization (e.g. Al III and Si IV) and those primarily produced by collisional ionization in cooling gas (e.g. C IV, N V and O VI). Unfortunately the IUE data for

N V toward the SN are too noisy to be of any value and IUE is unable to operate at those wavelengths needed to record O VI. Therefore, our assessment of possible changes in the behavior of line profiles will be restricted to Al III, Si IV and C IV.

In §IIIc we noted that between -20 and 120 km s^{-1} the prominent double peaked absorption structure seen for Si II and Al III is not as well defined in the Si IV and C IV profiles. This change appears to be the result of a progressive increase in the overall breadth of the features from Al III to Si IV to C IV. These differences are too large to be caused by changes in the Doppler broadening among the three ions at their favored temperatures from collisional ionization. For instance, the peak equilibrium abundances of C IV and Si IV occur near $T = 10^5$ and $0.8 \times 10^5 \text{ K}$, respectively (Shapiro and Moore 1976). At these temperatures, thermal Doppler broadening of C IV and Si IV would produce gaussian broadened line profiles with FWHM of 20 and 11 km s^{-1} , respectively. However, in non-equilibrium cooling as expected in a galactic fountain flow, the recombination of the gas proceeds more slowly than its cooling and the temperatures at which Si IV and C IV peak in abundance are somewhat reduced. Clearly a broadening of less than 20 km s^{-1} for C IV and less than 11 km s^{-1} for Si IV would be inadequate for explaining all the observed profile differences between Al III, Si IV and C IV.

The most surprising effect seen in the detailed profiles shown in Figures 3, 4 and 5 is that the Si IV profiles more closely resemble the smoother appearing C IV profiles than the sharper Al III profiles. From the theoretical considerations referred to above, one might expect the profile of the two species whose origin is expected to be dominated by photoionization (e.g. Al III and Si IV) to be roughly similar and to differ substantially from the profile for an ion expected to have an important contribution from cooling fountain gas (e.g. C IV). Additional concern for the behavior of Si IV with respect to C IV comes from an investigation of Figure 8 which shows the ratio of column densities as a function of velocity. In the velocity range of strong Milky Way absorption (i.e. from 0 to 100 km s^{-1}) the ratios of C IV and Si IV column densities range from about 3 to about 5 . If the physical processes producing the C IV (e.g. cooling fountain gas plus some photoionization) differ substantially from the processes which produce the Si IV (e.g. almost entirely photoionization) it is difficult to understand why the ratios of these ions should be so constant with velocity. While it appears that all the important atomic physics is included in the calculation of expected column densities in cooling fountain gas by Edgar and Chevalier (1986), we

wonder if errors in some of the assumed atomic process rates have produced an underestimate in the amount of Si IV expected in such a gas. Referring to Table 4, we see that an increase of the predicted Si IV column density of about a factor of 3 for the SN sight line would be required to make the calculations agree with the observed value.

If the observed C IV and Si IV ions are both formed in the evaporative interfaces between cool clouds and a hot medium in which they are imbedded, one might expect both ions to have similar line profiles which would be influenced by the velocity distribution of the cooler cloud material along the sight line but modified somewhat by thermal Doppler broadening and by the evaporative expansion of the cloud material in the hotter boundaries. In the case of evaporation, the ionization lags behind the heating. Therefore, ions such as C IV and Si IV will have their peak abundances at temperatures that are *higher* than in the equilibrium situation. For example, the non-equilibrium evaporation calculations by Bohringer and Hartquist (1987) for C IV show that the peak abundance of C IV occurs near 3 to 4×10^5 K rather than near the equilibrium value which is about 1×10^5 K. At such a high temperature the FWHM of a C IV absorption line due to thermal broadening alone would be about 35 to 40 km s⁻¹. This amount of broadening could explain much of the observed difference between the profiles of Al III and C IV in Figures 3 and 5. Unfortunately, as in the case of the cooling fountain gas, the non-equilibrium evaporative interface models predict a C IV to Si IV column density ratio of about 20 (Ballet et al. 1986) substantially larger than the observed ratio of 3 to 5.

In conclusion, while the actual column density estimates for C IV and Si IV in the Milky Way halo gas toward the SN are compatible with expectations based on previous work pertaining to the origin of Milky Way halo gas, we are troubled by the fact that the similarity in the profile of Si IV and C IV suggests to us a similar physical origin for these two species. This conflicts with the current theory, which suggests rather different origins for Si IV and C IV.

c) LMC Gas

The present data can be used to address two questions of great interest: 1) Do the IUE data provide clues about the nature of the interstellar medium local to the SN explosion into which the SN ejecta will eventually expand? and 2) Do the IUE data contain evidence for the ionization produced by the burst of EUV radiation which may have been produced by the SN explosion? In

order to begin to answer these questions we must first consider what is known about the gaseous environment of the SN and what absorption features might be expected for such an environment before the SN explosion occurred.

A visual inspection of deep, narrow-band images of the 30 Doradus region of the LMC obtained in the lines of $H\alpha$ and $[O III] \lambda 5007$ by Lasker (1971), Elliot et al.(1977) and Lortet and Testor (1984) reveals that SN 1987A occurred within the boundaries of the southwestern extension of the 30 Doradus nebula. The gaseous emission at the position of the SN is weaker than at the center of the nebula which lies 21 arc minutes away. However, the emission is still quite strong and exhibits a complex appearance which is a characteristic of the gas in 30 Doradus. An excellent CCD image of the $[O III]$ emission immediately around the SN obtained using a coronagraph is shown by d'Odorico (1987) who comments that the precursor star appears to have been located near the edges on a bright ridge of $[O III]$ emission which lies at the boundaries of a bubble. Although nebular emission line spectra have not yet been published, Danziger et. al. (1987) noted that the emission near the SN has the characteristics of a low density H II region with weak nitrogen lines.

The presence of $[O III]$ emission reveals the highly ionized character of the gas in the general vicinity of the SN. The creation of O III requires 35.1 eV which is similar to the 33.5 eV needed to photoionize Si III to Si IV. This implies that one might expect to measure substantial column densities of Si IV and perhaps even C IV along the sight line to the SN as a result of absorption by pre-existing H II region gas, depending, of course, on the exact position of the SN with respect to the dense clumps of H II region gas and whether or not the SN is in front of or behind these clumps. Information about the line of sight position of the SN can be inferred from the reddening to the SN which has been estimated to be $E(B-V) = 0.15$ (Fitzpatrick 1988). Approximately 0.07 magnitudes of this reddening is produced by the Milky Way (McNamara and Feltz 1980) with the remaining 0.08 magnitudes produced in the LMC. With the LMC hydrogen to $E(B-V)$ ratio appropriate for the 30 Doradus region from Fitzpatrick (1986) of 2.4×10^{22} atoms $\text{cm}^{-2}\text{mag}^{-1}$, an LMC reddening $E(B-V) = 0.08$ implies the SN is beyond about 1.9×10^{21} atoms cm^{-2} of H I. The H I 21 cm emission profiles of Rohlfs et. al. (1985) for positions near the SN give a total LMC H I column density of 2×10^{21} atoms cm^{-2} . The SN apparently lies beyond most of the neutral interstellar gas in the LMC (de Boer, Richtler and Savage 1987).

From the information above we conclude it is likely that relatively strong to very strong Al III, Si IV and C IV absorption will be produced by the pre-existing ISM in the direction of the SN. However, it is difficult to make a reliable estimate of the expected strength of this absorption because the ISM in the direction of the SN is so patchy. Some very rough guidance might be provided by IUE interstellar absorption line measurements toward the three objects R136a (de Boer, Koornneef and Savage 1980; de Boer, Fitzpatrick and Savage 1985), R144 (de Boer and Savage 1980), and HD36402 (deBoer and Nash 1982) whose Al III, Si IV and C IV profiles are shown Figure 9. R136a lies at the center of the 30 Doradus nebula and has $E(B-V)_{LMC}$ of about 0.30. R144 lies about 4.3 arc min from center of the nebula and has $E(B-V)_{LMC}$ of about 0.09 (Fitzpatrick and Savage 1984). HD 36402 lies in a roughly spherical H II region of approximately 100 pc diameter located about 2° from R136a which places it well beyond the boundaries of the 30 Doradus nebula and has a small $E(B-V)_{LMC}$ (see deBoer and Nash 1982). In the progression from R136a to R144 to HD 36402, the Si IV and C IV absorption lines at LMC velocities progress from exceptionally strong to moderately strong. One might expect the data for the SN sight line to represent an intermediate case. However, we are unable to predict whether the absorption line strengths will lie closer to the exceedingly strong R136a case or the moderately strong R144 case.

The expected velocity of the Al III, Si IV and C IV absorption produced by H II region gas will depend on the gas kinematics near the site of the SN. It is well documented that the gas motions in the 30 Doradus region are violent and complex and there can be large variations from one position to the next (Elliott et al.1977; Meaburn 1984). Y. H. Chu (private communication) has obtained a long slit high resolution echelle spectrum of a position 10" south of SN 1987A with an east-west slit orientation extending approximately 65" west and 130" east. The spectrum which includes the nebular emission lines of $H\alpha$ λ 6563 and [N II] $\lambda\lambda$ 6584 and 6548 was obtained 7 January 1988 (UT) with the echelle spectrograph on the CTIO 4 m telescope, the air Schmidt camera and the GEC 385x576 element CCD. The strong telluric $H\alpha$ emission feature gives us a zero point in the velocity scale and indicates that the 1.64" slit width provided a spectral resolution of 21 km s^{-1} FWHM. The SN measurements were part of a program to study SN remnants in the Magellanic Clouds. Details about the instrument configuration and the reduction techniques are given in Chu and Kennicutt (1988). The resulting spectrum shows strong $H\alpha$ and weak [N II] emission from

the general H II region gas of the outlying parts of the 30 Doradus nebula. The correction to heliocentric velocity at the time of observation is $v_{\text{obs}} - v_{\text{Helio}} = 0.57 \text{ km s}^{-1}$. Although there is some irregularity in the strength and velocity of the strong H α emission along the slit, the general H II region heliocentric velocity over the region from 30" west to 50" east is $270 \pm 2 \text{ km s}^{-1}$. At selected positions along the slit other velocity components of emission are apparent. For example, strong H α emission at 310 km s^{-1} is apparent at a position along the slit extending from approximately 10" to 30" west. The extracted H α spectrum for a 10.8" long region along the slit closest to the SN is shown in Figure 10. The nebular H α is centered at 270 km s^{-1} and has a measured full width at half intensity of 47 km s^{-1} , a number which is only slightly affected by instrumental resolution. At 1/10 intensity the nebular H α can be traced from 230 to 310 km s^{-1} .

Based on the H α profile of Figure 10 and the assumption that H II region absorbing gas of similar kinematic properties lies *in front* of the SN we might expect strong Al III, Si IV and C IV absorption from the general H II region to have its maximum absorption centered near 270 km s^{-1} and to have lines with full widths at half intensity of roughly 45 km s^{-1} . The observed profiles of Al III, Si IV and C IV seem well described by this prediction.

In the case of the neutral gas, the H I 21 cm emission line measurements of Rohlfs et al. (1984) for two positions near the SN are illustrated in de Boer, Richtler and Savage (1987). These data indicate that the bulk of the H I gas in the direction of the SN has a two component velocity structure peaking near v_{Helio} of 245 and 280 km s^{-1} but with detectable emission extending over the range from approximately 200 to 340 km s^{-1} .

We conclude from the discussion above that we would expect the pre-existing environment of the SN to produce Al III, Si IV and C IV absorption ranging from moderately strong to very strong and centered at a velocity of approximately 270 km s^{-1} . This absorption will therefore represent a major source of confusion in our attempts to understand the modifications of the surrounding medium produced by the SN EUV flash.

In addition, there is some evidence that there may be a substantial amount of gas at temperatures well above the range needed to collisionally ionize Al, Si and C to the levels we observe. Pettini et al. (1988) have reported an absorption feature which could be the [Fe X] $\lambda 6374.1$ transition over radial velocities between 215 and 270 km s^{-1} . Unfortunately, absorption in the diffuse interstellar band known to exist near 6379.30 \AA will blend with the absorption

identified as being produced by Fe X. If the substance producing the diffuse band is present in the Milky Way matter in the direction of the SN, it could explain much of what is observed. If the feature is due to Fe X, the lack of any observed change in the strength of the feature over a time scale of several months argues against the interpretation that the ions were created impulsively by the supernova flash in a dense region very near the explosion. Instead, collisionally ionized gas (at $T \sim 10^6$ K) over a volume several hundred pc to a kpc in diameter may explain the presence of 3×10^{16} Fe X ions cm^{-2} , but this material must be behind nearly all of the foreground neutral hydrogen in order to explain the lack of a very strong source of soft X-rays in this part of the sky (Marshall and Clark 1984; Singh et al. 1987). In view of the enormous pressure ($p/k > 10^6 \text{ cm}^{-3}$ K) and radiative loss rates associated with the volume of hot gas, we should not be surprised to find substantial abundances of Al III, Si IV and C IV.

d) Circumstellar Environment of the Supernova

The immediate surroundings of the supernova contain gaseous material expelled by the precursor star at various stages of evolution. When the star was a red supergiant, a slow wind probably created a large (~ 10 pc diameter) spherical volume of material centered on the star. Somewhere within the innermost parsec of this sphere, the much faster and lower density wind from the more recent blue supergiant phase swept up the wind from the cool star and compressed it into a thin, dense shell (Chevalier 1988). When the supernova exploded, the gas within this shell was ionized abruptly by the enormous impulse of ultraviolet photons created when the outermost portion of the supernova's envelope was heated to $T \sim 10^{5.35}$ K by the emergence of the shock from the interior (Dopita et al. 1987; Woosley 1988). Several months later, UV and visible emission lines from atoms in the densest portions of this compact shell became evident (Wamsteker et. al. 1987; Kirshner et. al. 1987) at a heliocentric velocity of approximately 280 km s^{-1} and with a FWHM of about 30 km s^{-1} (Fransson et al. 1988). The analysis of these data showed that the ejected material is especially rich in nitrogen -- an indication that significant loss of the outer hydrogen envelope may have occurred in the star's earlier stages of evolution. Moreover, ratios of different emission line strengths indicated a characteristic density of electrons $n_e = 2 \times 10^4 \text{ cm}^{-3}$ (Fransson et al. 1988) and temperature $T = 5.5 \times 10^4 \text{ K}$ (Wampler and Richichi 1988). The angular extent of the region emitting the UV lines was not resolved by the IUE spectrograph, which indicates the radius of the dense shell must be less than 0.3 pc. The fact that some of the lines were still growing in strength about a year after the explosion (due to light travel time effects) demonstrates that the shell must not be significantly smaller than 0.3 pc. Fransson et. al. gave a very approximate estimate for the mass of the emitting material; their value of $0.05 M_{\odot}$ is roughly consistent with the expected amount of gas from both the blue and red star winds within several tenths of a pc from the supernova.

In principle, UV absorption lines could provide additional information on the abundances and physical character of gases very near the supernova. Unfortunately, nearly all of these circumstellar lines are completely swamped by the very broad features created by the much larger amount of foreground gas associated with the LMC. Our only hope in bypassing the effects of the more pervasive gas at approximately the same doppler shift is to rely on absorption features from excited fine structure levels of various atoms. Under the right circumstances these absorption features may strongly favor the circumstellar gas, since the excited levels are populated either by collisions in regions of high density

and temperature, or by optical pumping through higher electronic states in the presence of intense ambient radiation fields (Spitzer and Jenkins 1975).

The most conspicuous UV lines from fine-structure levels are those from the upper level of C II. In an H II region at a temperature $10^3 \leq T \leq 10^4$ K, an electron density $n_e \sim 30 \text{ cm}^{-3}$ is sufficient to create an excited C II population equal to that of the ground level. The relative ease in creating C II*, together with the high cosmic abundance of carbon, explains why we see C II* over a broad range of velocities (more than 100 km s^{-1}) centered on 270 km s^{-1} . Evidently we are still registering the presence of foreground ionized (and possibly even neutral) gases associated with the LMC.

Lines from Si II* are more difficult to produce. Within any H II region of low density, collisions with electrons will create a ratio of Si II* to Si II which is 17 times lower than that of C II* to C II -- a fact supported by the profiles shown in Figure 1. For optical pumping the disadvantage is much less. Si II has a number of very strong UV transitions from the ground state. It follows that Si II* should allow us to discriminate better the circumstellar absorptions from features produced by the more extensively distributed material in the LMC. Hence, we shall rely on the Si II* absorptions (or lack thereof) to probe the environment near the supernova. For our interpretation of the Si II* lines, we first need to predict how many of the nearby Si atoms escape being ionized to higher levels by the UV photons from the supernova. A B3 Ia star produces $10^{45.57}$ Lyman limit photons s^{-1} (Panagia 1973). This rate is about a factor 25 below that needed to maintain full ionization of $0.05 M_{\odot}$'s of hydrogen at a density $n_e = 2 \times 10^4 \text{ cm}^{-3}$. Therefore, provided the dense shell surrounding the supernova is reasonably intact (i.e., it has not broken into thin filaments with large gaps in between), most of the hydrogen within and outside the shell must have been neutral prior to the outburst.

Nearly all of the Si atoms coexisting with the neutral hydrogen would be singly ionized. Initially, the Si⁺ would be shielded from most of the supernova's ionizing radiation ($E > 16.34 \text{ eV}$) by intervening neutral hydrogen. At a distance r from the supernova, we expect that only after a time delay $t(r)$ satisfying

$$4\pi \int_0^{t(r)} \int_{13.60 \text{ eV}}^{\infty} N_E(t) r^2 \sigma(t) dE dt = N_H(r) \quad (3)$$

will the ionization front eat its way through an interior volume containing $N_H(r)$ hydrogen atoms, either within the shell or in the surrounding, undisturbed medium, and thereafter expose the Si II atoms to the ionizing photons. For simplicity, we assume that the expanding supernova envelope radiates as a perfect

black body, yielding a photon energy spectrum

$$N_E(t) = \frac{9.89 \times 10^{22} E^2}{\exp[11605 E/T_e(t)] - 1} \quad (\text{photons cm}^{-3} \text{ s}^{-1} \text{ erg}^{-1}) \quad (4)$$

To define the evolution of this flux with time, we adopted the effective temperature $T_e(t)$ from

Woosley's (1988) model 10H and calculated the envelope's radius $r_*(t) = [L(t) / 4\pi\sigma T_e^4(t)]^{1/2}$.

Another simplification of our analysis is that the thickness of the front is assumed to be infinitesimal and that the hydrogen ahead of it is perfectly opaque to all photons with $E > 13.60$ eV. For the short time scale which applies to this problem, there are virtually no recombinations of the ions or hydrodynamic adjustments behind the front.

Once the ionization front has past beyond any given point, the local Si^+ is exposed to all of the subsequent ionizing photons and has a survival probability,

$$P(r) = \exp \left[- (r_*/r)^2 \int_{t(r)}^{\infty} \int_{16.34 \text{ eV}}^{\infty} N_E(t) \sigma(E) dE dt \right] \quad (5)$$

where the photoionization cross sections $\sigma(E)$ for Si^+ are those calculated by Reilman and Manson(1979).

Virtually all of the Si atoms within the dense shell are ionized by the UV photons from the supernova. Beyond the shell, the undisturbed wind created long ago by the red supergiant has a hydrogen density

$$n(\text{H}) = 3.20 \times 10^6 \frac{\dot{M}}{r^2 v_w} \quad (\text{cm}^{-3}), \quad (6)$$

where the mass loss rate \dot{M} is expressed in $M_{\odot} \text{ yr}^{-1}$, r in pc, and the velocity of the wind v_w in km s^{-1} . For any reasonable values of \dot{M} and v_w , $n(\text{H})$ is too low to collisionally excite the Si II fine structure levels for r greater than a few tenths of a pc. However radiation from the supernova will excite the very strong ultraviolet transitions of Si II and optically pump the fine-structure levels of the ground electronic state. In the context that the pumping lines are optically thin, Flannery, Rybicki and Sarazin (1980) calculated that at a distance r from a spherical source of radius r_* emitting F_{ν} $\text{ergs cm}^{-2} \text{ s}^{-1} \text{ Hz}^{-1}$

an equilibrium ratio

$$\frac{N(\text{Si II}^*)}{N(\text{Si II}_{\text{total}})} = \frac{0.678 \xi}{1 + 1.017 \xi} \quad (7)$$

will be established, where

$$\xi = 8.79 \times 10^{12} \left[\frac{r^*}{r} \right]^2 F_V \quad (8)$$

(If the Si II is optically thick, the optically thin approximation must still apply in the inner part of the zone, and the thickness of this zone is sufficient to produce observable Si II lines if the velocity dispersion is not markedly less than the instrumental resolution of IUE.) The time constant for establishing the equilibrium is governed by the inverse of the spontaneous decay rate A_{21} of the upper fine-structure level, which for Si II amounts to 1.3 hours. Since this time is short compared to the interval over which the flux could appreciably change at the time of observation, the equilibrium calculation should be valid.

Near the middle of the time interval over which the shortest wavelength portions of the spectrum were observed (the first four images listed in Table 1), Kirshner et. al. (1987) found that the apparent flux of the supernova was about $1.1 \times 10^{-23} \text{ erg cm}^{-2} \text{ s}^{-1} \text{ Hz}^{-1}$ at wavelengths covering some of the strongest Si II lines. To convert this flux into an estimate at a representative distance of 1 pc, we need to compensate for the attenuation of the UV flux by foreground dust, in addition to multiplying the apparent flux by the square of the distance to the supernova, $(5 \times 10^4 \text{ pc})^2$. Fitzpatrick (1988) estimates that the total reddening $E(B - V)$ toward the supernova is 0.15, of which 0.07 is created by material in our galaxy. If we assume $E(1250\text{\AA} - V)/E(B - V) = 6.6$ in our galaxy (Savage and Mathis 1979) and 8.0 in the LMC¹ (Fitzpatrick 1986) and consider that $A_V / E(B - V) = 3.1$ in both regions, we calculate that "dereddening" the flux should amount to an increase by a factor 4.2, making the real flux at 1 pc equal to $1.2 \times 10^{-13} \text{ erg cm}^{-2} \text{ s}^{-1} \text{ Hz}^{-1}$ and $\xi = 1.0$.

The abundance $A(\text{Si})$ of atomic silicon to hydrogen in the circumstellar gas is probably considerably lower than the solar abundance ratio, since the ratio of heavy elements to hydrogen in the LMC is lower than that of our galaxy. Also, some of the Si may be depleted onto grains. Some insight on $A(\text{Si})$ in

¹ The value could be as large as 10 if the supernova has dust which is more characteristic of that in front of stars associated with the 30 Dor nebula.

LMC gases is available from our plot of the apparent optical depth of the line at 1808 Å. An integration of τ over the range $190 < v < 320 \text{ km s}^{-1}$ (see Fig. 2). leads to a formal result for the column density $N(\text{Si II}) = 3.5 \pm 0.3 \times 10^{15} \text{ cm}^{-2}$. Unlike the profiles of the highly ionized species, however, we have no assurance that unresolved, deeply saturated structures within the profiles are not misleading us into underestimating the amount present. Moreover, many of the Si atoms in H II regions which are excited by very hot stars may be doubly or triply ionized. Thus, our inferred abundance $A(\text{Si})$ taken from $N(\text{Si II})/N(\text{H}) = 2 \times 10^{-6}$ is actually a lower limit. Here, $N(\text{H})$ was taken to be $2 \times 10^{21} \text{ cm}^{-2}$ (see §IVc).

One might question whether or not $A(\text{Si})$ in the circumstellar wind could be different from the generally distributed material in the LMC because grains are created efficiently but the material has not yet been exposed to the usual destructive processes. On the one hand, a study of the mass-loss envelopes of a diverse collection of M giants in our galaxy by Knapp (1985) indicates that there are no anomalies in the gas-to-dust ratios. On the other hand, observations of very weak thermal SiO emission in the outer portions of such envelopes by Morris et al. (1979) indicated that perhaps less than 1% of the Si may have escaped being consolidated into grains. It is difficult to say whether or not this high efficiency in depleting the gas-phase Si is maintained for the modified abundances in the circumstellar gas of the supernova progenitor.

Incorporating the principles discussed above, we arrive at our net expectation for the column density of Si II* through the immediate neighborhood of the supernova,

$$N(\text{Si II}^*) = \int_{r_*}^{\infty} n(\text{H}) A(\text{Si}) P(r) \frac{N(\text{Si II}^*)}{N(\text{Si II}_{\text{total}})} dr \quad (9)$$

The greatest concentration of Si II* is at about 1 or 3 pc from the supernova; very few of the Si atoms remain in the singly ionized form within the dense shell. Table 5 summarizes the results of Eq. 9 for several values of \dot{M}/v_w . The numbers clearly show that the dependence of $N(\text{Si II}^*)$ on \dot{M}/v_w is much steeper than linear. The principal cause of this effect is that the additional material slows down the ionization front in the critical region where optical pumping is important. The resulting delay shields the Si atoms from the largest dose of hard, ionizing radiation which occurs at the very beginning. A factor of 2 change in ξ for appropriate values of \dot{M}/v_w seems to change the resultant $N(\text{Si II}^*)$ by a relatively small amount.

The tracings in Fig. 1d reveal a moderately significant absorption feature due to Si II* at 1264.74 Å at a velocity near that of the material in the LMC. Corresponding features are not evident for the two other Si II* lines ($\lambda\lambda$ 1309.27 and 1533.45) because these transitions are not as strong. Assuming that the 1264.74 Å line is completely unsaturated, our measured equivalent width of 67 ± 20 mÅ yields a column density $N(\text{Si II}^*) = 5.5 \times 10^{12} \text{ cm}^{-2}$. The velocity centroid of the profile is at $255 \pm 6 \text{ km s}^{-1}$. While we expect outflowing circumstellar material to have an absorption velocity slightly more negative than most of the gas which can be seen in emission, our displacement of -25 km s^{-1} seems rather large.

It is likely that nearly all of the Si II* we have registered belongs to a foreground H II region in the LMC, and indeed the velocity we measured is approximately consistent with this interpretation. Also, we calculate that at a temperature of 10^4 K , an H II region containing the amount of Si II* that we derived should have an emission measure of $600 \text{ cm}^{-6} \text{ pc}$, assuming, as before, that $\text{Si}/\text{H} = 2 \times 10^{-6}$ in the LMC. The telluric H α recorded by Y.H. Chu and shown in Fig. 10 can be used to estimate the intensity of the much stronger nebular H α emission near 270 km s^{-1} . At the time of observation the expected intensity of the telluric line based on the H α models of Anderson et al. (1987) is approximately 6.5 Rayleighs. This number assumes solar maximum conditions, which according to J. Harlander (private communication) provide better agreement between the model predictions and recent direct measures of the telluric H α emission. Therefore, the nebular 270 km s^{-1} H α emission, which is 25 times stronger than the telluric line, has an intensity corresponding to about 160 Rayleighs. Assuming that the H α emission is optically thin and gives 0.243 Rayleighs for $1 \text{ cm}^{-6} \text{ pc}$ at $T = 10^4 \text{ K}$ (Osterbrock 1974), this implies a nebular emission measure of $660 \text{ cm}^{-6} \text{ pc}$.

From the above argument, we propose that Si II* absorption from gas very near the supernova is of order or less than about half the total column density we detected at 255 km s^{-1} . For $\xi = 1$, the numbers in Table 5 indicate that a conservative upper limit for any mass-loss material which is outside the dense shell gives a density less than that of a wind having $\dot{M} / v_w \sim 1 \times 10^{-6} M_\odot \text{ yr}^{-1} (\text{km s}^{-1})^{-1}$. Our upper limit rules out the upper end of the range of observed mass loss rates for cool, giant stars (e.g. Bowers 1985; Knapp 1985) such as those found for the OH/IR maser emission stars (Herman 1985).

If the dense shell of gas which is responsible for the emission lines contains $0.05 M_\odot$ at a distance of 0.3 pc, its column density of hydrogen $N(\text{H})$ would be $6 \times 10^{18} \text{ cm}^{-2}$. On top of it one could add $3 \times 10^{19} \text{ cm}^{-2}$ for the undisturbed wind material. Note that for our limit for \dot{M} / v_w , the mass of

material piled up at $r = 0.3$ pc works out to $0.3M_{\odot}$. From Eq. 6, the volume density just outside the shell should be $\leq 35 \text{ cm}^{-3}$, with an inverse-square law decrease at greater distances. This amount of gas is substantially lower than the uniform value of 1000 cm^{-3} assumed by Raga (1987), who proposed that most of the C IV and Si IV appearing at the LMC velocity in the supernova spectrum was created by flash photoionization of the surrounding material. Quite apart from any specific model for the creation of Si IV very near the supernova, we find that if we multiply our inferred total column density for circumstellar gas by our adopted $A(\text{Si})$, we arrive at $N(\text{Si}) = 7.2 \times 10^{13} \text{ cm}^{-2}$ -- a value which is lower than our observed *lower limit* for $N(\text{Si IV})$ for gas at velocities near that of the supernova (see Table 3). Likewise, if the abundance of carbon in the circumstellar material is less than 1/10 the solar value, more than 40% of the C would need to be triply ionized if $N(\text{C IV})$ equaled our lower limit of $10^{14.81} \text{ cm}^{-2}$ deduced from the 1550.77 Å line. This statement is probably much too conservative, since the real column density of C IV is very likely to be substantially greater than our formal lower limit.

In addition to absorptions from Si II*, we could in principle also look for evidence of excited neutral oxygen atoms. O I has two excited fine-structure levels, however for the 1302 Å multiplet only the upper member of the two levels is free from interference by another line (the 1304 Å line of Si II). The UV transitions which can pump O I are considerably weaker than those of Si II, however this is compensated by the much lower spontaneous decay rate A_{21} . For a given amount of gaseous material, the visibility of O I is roughly equivalent to that of Si II, and the higher cosmic abundance of oxygen is balanced by the fact that the transition we can view is much weaker. The main drawback which makes O I** less sensitive than Si II* in our search for circumstellar material is that the statistical weight of the upper level of O I is only 1/9 of the total for all three levels, as opposed to 2/3 for the excited level of Si II. Thus, we do not gain by including O I**.

Summarizing, our analysis of the essential features in the interstellar spectra at LMC velocities suggest that the absorption is dominated by gas which was present in the vicinity of Sk -69 202 before the star became SN 1979A. The strengths and the velocity structure in the lines of C IV, Si IV and Si II* are compatible with absorption by normal H II region gas.

We thank the IUE observatory staffs at the Goddard Space Flight Center and at the ESA IUE ground station for their help in acquiring and processing the IUE satellite data for SN 1987A. The very rapid

response of the IUE observatory staff to the first announcement of the explosion made this project possible. We acknowledge the very helpful assistance of Marilyn Meade with the processing of the SN high dispersion data on the computing facilities of the Midwest Astronomical Data Reduction and Analysis Facility in Madison. The $H\alpha$ data kindly provided by Y. H. Chu of the University of Illinois were particularly valuable in evaluating the possibility of blending between absorption produced in the circumstellar environment of the SN and absorption produced in the extensive H II region in the general direction of the SN. We appreciate the help provided by J. Harlander of the University of Wisconsin in estimating the expected strength of the terrestrial $H\alpha$ line, a result we used in determining the nebular line intensity. The work of BDS was supported through NASA grant NAG-186. EBJ and CLJ at Princeton were supported by NASA grant NAG5-1004.

REFERENCES

- Anderson, D.E., Meier, R.R., Hodges, R.R., and Tinsley, B.A. 1987, *Jour. Geo. Res.*,
92 No.A7, 7619.
- Ballet, J., Arnaud, M., and Rothenflug, R. 1986, *Astr. Ap.*, 161, 12.
- Blades, J.C., Wheatley, J. M., Panagia, N., Grewing, M. Pettini, M., and Wamsteker, W.
1988, *Ap. J.*, (in press).
- Boggess, A. et. al. 1978a, *Nature*, 275, 372.
_____. 1978b, *Nature*, 275, 377.
- Bohringer, H., and Hartquist, T.W. 1987, *M.N.R.A.S.*, 228, 915.
- Bowers, P. F. 1985, in *Mass Loss from Red Giants*, eds. M. Morris and B. Zuckerman,
(Dordrecht: Reidel), p.189.
- Bregman, J.N. 1980, *Ap.J.*, 236, 577.
- Bregman, J.N., and Harrington, P.J. 1986, *Ap.J.*, 309, 833.
- Chevalier, R. A. 1988, *Nature*, 332, 514.
- Chevalier, R. A., and Fransson, C. 1984, *Ap.J. (Letters)*, 279, L43.
- Chu, Y.H., and Kennicutt, R.C. 1988, *A.J.*, 95, 1111.
- Danziger, I.J., Fosbury, R.A.E., Alloin, D., Cristiani, S., Dachs, J., Gouiffes, C., Jarvis, B.,
and Sahu, K.C. 1987, *Astr. Ap.*, 177, L13.
- de Boer, K.S., Fitzpatrick, E.L., and Savage, B.D. 1985, *M.N.R.A.S.*, 217, 115.
- de Boer, K.S., Grewing, M., Richtler, T., Wamsteker, W., Gry, C., and Panagia, N.
1987, *Astr. Ap.*, 177, L37.
- de Boer, K.S., Koornneef, J., and Savage, B.D. 1980, *Ap. J.*, 236, 769.
- de Boer, K.S., and Nash, A. 1982, *Ap.J.*, 255, 447.
- de Boer, K.S., Richter, T., and Savage, B.D. 1987, in *ESO Workshop on SN1987A*,
ed. I. Danziger, p.549.
- de Boer, K. S., and Savage, B.D. 1980, *Ap. J.*, 238, 86.
_____. 1983, *Ap.J.*, 265, 210.
- d Odorico, S. 1987, *The ESO Messenger*, 49, 34.
- Dopita, M. A., Meatheringham, S. J., Nulsen, P., and Wood, P. R. 1987, *Ap. J. (Letters)*, 322, L85.

Dupree, A. K., Kirshner, R. P., Nassiopoulos, G. E., Raymond, J. C., and Sonneborn, G. 1987, *Ap. J.*, **320**, 597.

Dupree, A. K., and Raymond, J. C. 1983, *Ap. J. (Letters)*, **275**, L71.

Edgar, R. J., and Chevalier, R. A. 1986, *Ap. J. (Letters)*, **310**, L27.

Elliot, K. H., Goudis, C., Meaburn, J., and Tebbut, N. J. 1977, *Astr. Ap.*, **55**, 187.

Evans, N. R., and Imhoff, C. L. 1985, *IUE NASA Newsletter*, **28**, 77.

Fitzpatrick, E. L. 1986, *A. J.*, **92**, 1068.

_____. 1988, submitted.

Fitzpatrick, E. L., and Savage, B. D. 1983, *Ap. J.*, **267**, 93.

_____. 1984, *Ap. J.*, **279**, 578.

Flannery, B. P., Rybicki, G. B., and Sarazin, C. L. 1980, *Ap. J. (Suppl.)*, **44**, 5 39.

Fransson, C., Cassatella, A., Gilmozzi, R., Panagia, N., Wamstecker, W., Kirshner, R. P., and Sonneborn, G. 1988, *Ap. J.*, (submitted).

Fransson, C., and Chevalier, R. A. 1985, *Ap. J.*, **296**, 35.

Hartquist, T. W., Pettini, M., and Tallant, A. 1984, *Ap. J.*, **276**, 519.

Herman, J. 1985, in *Mass Loss from Red Giants*, eds. M. Morris and B. Zuckerman, (Dordrecht: Reidel), p. 215.

Jenkins, E. B. 1978, *Ap. J.*, **220**, 107.

_____. 1987, in *Exploring the Universe with the IUE Satellite*, eds. Y. Kondo et al. (Dordrecht: Reidel), p. 531.

Kaelble, A., de Boer, K. S., and Grewing, M. 1985, *Astr. Ap.*, **143**, 408.

Kirshner, R. P., Sonneborn, G., Crenshaw, D. M., and Nassiopoulos, G. E. 1987, *Ap. J.*, **320**, 602.

Knapp, G. R. 1985, *Ap. J.*, **293**, 273.

Lasker, B. 1971, *CTIO Contribution No. 127*.

Loret, M. C., and Testor, G. 1984, *Astr. Ap.*, **139**, 330.

Magain, P. 1987, *Nature*, **329**, 606.

Marshall, F. J., and Clark, G. W. 1984, *Ap. J.*, **287**, 633.

Martin, C., and Bowyer, S. 1987, *B.A.A.S.*, **18**, 1036.

McNamara, D. H., and Feltz, K. A. 1980, *Pub. A.S.P.*, **92**, 587.

- Meaburn, J. 1984, *M.N.R.A.S.*, **211**, 521.
- Morris, M., Redman, R., Reid, M. J., and Dickinson, D. F. 1979, *Ap. J.*, **229**, 257 .
- Morton, D.C., and Smith, W. H. 1973, *Ap. J.(Suppl.)*, **26**, 333.
- Osterbrock, D. 1974, *Astrophysics of Gaseous Nebulae*, (San Francisco:Freeman).
- Panagia, N. 1973, *A. J.*, **78**, 929.
- Pettini, M., and West, K.A. 1982, *ApJ.*, **260** , 561.
- Pettini, M., Stathakis, R., D'Odorico, S., Molaro, P., and Vladilo, G. 1988, *Ap. J.*, in press.
- Raga, A. C. 1987, *A. J.*, **94**, 1578.
- Reilman, R.F., and Manson, S.T. 1979, *Ap. J. (Suppl.)*, **40**, 815.
- Rohlf, K., Kretschmann, J., Siegman, B.C., and Feitzinger, J.V. 1984, *Astr. Ap.*, **137**,343.
- Routly, P. M., and Spitzer, L. 1952, *Ap. J.*, **115**, 227.
- Savage, B.D. 1987, in *Interstellar Processes*, eds. D.J.Hollenbach and H.A.Thronson,
(Dordrecht:Reidel), p.123.
- _____ .1988, in *QSO Absorption Lines: Probing the Universe*, eds.J.C.Blades, D.Turnshek, and
C.A.Norman, (Cambridge:Cambridge U. Press), p.195.
- Savage, B.D., and deBoer, K.S. 1979, *Ap.J. (Letters)* , **230**, L77.
- _____ . 1981, *Ap.J.* , **243**,460.
- Savage, B.D., and Massa, D. 1987, *Ap.J.* , **314**, 380.
- Savage, B. D., and Mathis, J. S. 1979, *Ann. Rev. Astr. Ap.*, **17**, 73.
- Savage, B.D., and Meade, M. 1989, (in preparation).
- Shapiro, P.R., and Field, G.B. 1976, *Ap.J.* , **205**, 762.
- Shull, J. M., Snow, T. P., and York, D. G. 1981, *Ap. J.*, **246**, 549.
- Singh, K. P., Nousek, J. A., Burrows, D. N., and Garmire, G. P. 1987, *Ap. J.*, **313**, 185.
- Songaila, A., Blades, J.C., Hu, E.M., and Cowie, L. L.1986, *Ap.J.*, **303**, 198.
- Spitzer, L., and Jenkins, E. B. 1975, *Ann. Rev. Astr. Ap.*, **13**, 133.
- Turnrose, B.E., and Thompson, R.W. 1984, *IUE Image Processing Information Manual
Version 2.0* , (Computer Sci. Corp: TM-84/6058).
- Vidal-Madjar, A., Andreani, P., Cristiani, S., Ferlet, R., Lanz, T., and Vladilo, G. 1987,
Astr. Ap.,**177**,L17.

Wampler, E.J., and Richichi, A. 1988, *The ESO Messenger* , 52,14.

Wamsteker, W., Panagia, N., Barylak, M., Cassatella, A., Clavel, J., Gilmozzi, R., Gry, C.,
Lloyd, C., van Santvoort, J., and Talavera, A. 1987, *Astr. Ap.*, 177, L21.

Woolley, S. E. 1988, *Ap. J.*, (in press).

KLASS S. DE BOER: University of Bonn, Sternwarte, Auf dem Huegel 71, D 5300 Bonn,
West Germany

EDWARD B. JENKINS and CHARLES L JOSEPH: Princeton University Observatory, Peyton
Hall, Princeton University , Princeton, NJ 08544

BLAIR D.SAVAGE: Department of Astronomy, University of Wisconsin, 475 N. Charter Street,
Madison, WI 53706

TABLE 1
HIGH DISPERSION IUE ECHELLE SPECTRA OF SN 1987A

Image No.	Exp. time (min)	Date (UT time) (hr:min)	Ground ^a Station	wavelengths (velocity shift) ^b Angstroms (km s ⁻¹)	comment ^c
SWP 30377	14	Feb 24 (21:37)	G	1230 to 1800 (-4); 1800 to 1900 (0)	image saturation for $\lambda > 1900 \text{ \AA}$
SWP 30379	14	Feb 25 (00:53)	G	1230 to 1860 (0)	image saturation for $\lambda > 1860 \text{ \AA}$
SWP 30381	30	Feb 25 (04:24)	V	1230 to 1800 (0)	image saturation for $\lambda > 1800 \text{ \AA}$
SWP 30383	45	Feb 25 (08:09)	V	1230 to 1800 (0)	image saturation for $\lambda > 1800 \text{ \AA}$
SWP 30384	11	Feb 25 (09:30)	V	1808 (-5); 1854 (-4); 1862(0)	weak signal for $\lambda < 1700 \text{ \AA}$
SWP 30389	25	Feb 25 (21:17)	G	1808 (-5); 1854 (-3)	weak signal for $\lambda < 1700 \text{ \AA}$
SWP 30394	40	Feb 26 (04:14)	V	1808 (-1); 1854 (+3); 1862(+5)	weak signal for $\lambda < 1700 \text{ \AA}$
SWP 30399	75	Feb 26 (13:44)	V	1808 (-4); 1854 (+5); 1862(+7)	weak signal for $\lambda < 1700 \text{ \AA}$
LWP 10190	1.83	Feb 24 (22:14)	G	2000 to 3100 (-18)	
LWP 10192	1.67	Feb 25 (00:45)	G	2000 to 3100 (-18)	
LWP 10194	5	Feb 25 (05:30)	V	2000 to 2700 (-10)	image saturation for $\lambda > 2700 \text{ \AA}$
LWP 10196	8	Feb 25 (07:52)	V	2000 to 2700 (-8)	image saturation for $\lambda > 2700 \text{ \AA}$

^a Images from both the Goddard (G) and Vilspa (V) ground stations were utilized in this study.

^b We list the wavelength regions for which the various spectra were useful in our analysis and in parenthesis list the velocity shifts in km s⁻¹ needed to bring the various spectra into proper velocity registration .

^c The different spectra vary considerably in quality and wavelength coverage. The SN faded very rapidly over the first few days of observations and reasonably complete wavelength coverage was only obtained with the early spectra.

TABLE 2
UV Absorption Lines Illustrated in Figure 1

ion	f ^a	wavelength ^b	Echelle order	Figure	Notes
Al III	0.268	1862.795	74	1a	
Al III	0.539	1854.720	74	1a	
Si IV	0.262	1402.769	98	1a	
Si IV	0.528	1393.755	99	1a	
C IV	0.097	1550.774	89	1a	1
C IV	0.194	1548.202	89	1a	1
O I	0.0486	1302.169	106	1b	2
Si II	0.0055 ^c	1808.003	76	1b	
Si II	0.147 ^c	1304.369	106	1b	2
Si II	0.23 ^c	1526.719	90	1b	
Si II	0.959	1260.418	109	1b	
C II	0.118	1334.532	103	1b	3
Mg I	1.77	2852.127	81	1c	
Mg II	0.295	2802.704	82	1c	
Mg II	0.592	2795.528	83	1c	4
Al II	1.88	1670.786	82	1c	
Fe II	0.0395	2373.733	97	1c	
Fe II	0.203	2599.395	89	1c	5
Si II*	0.860	1264.730	109	1d	
Si II*	0.147	1309.274	105	1d	
Si II*	0.076	1533.445	90	1d	
C I	0.081	1560.310	88	1d	6
C I	0.136	1656.928	83	1d	6
Ni II	0.068	1741.560	79	1d	

^a f values are from Morton and Smith (1973) except as noted.

^b λ 's are in vacuum for $\lambda < 2000$ and in air for $\lambda > 2000$.

^c f values from Shull, Snow and York (1981).

NOTES TO FOLLOW TABLE 2

- NOTES.-- (1) Absorption by both components of the C IV doublet appear on each plot. Note that the slight difference in appearance in the same component from one plot to the next is the result of binning the data at slightly different velocities in each plot.
- (2) Si II λ 1304 absorption is situated near the O I λ 1302 absorption.
- (3) Absorption by C II* λ 1335.71 overlaps absorption by C II λ 1334.532. However, the LMC C II* absorption is free of contamination.
- (4) Absorption by both lines of the Mg II doublet appear on each plot.
- (5) The features to the left and right of Fe II λ 2599 are Mn II λ 2593.731 and λ 2605.697, respectively.
- (6) The lines of C I are actually complex overlapping blends of absorption from C I, C I* and C I**. See Morton and Smith (1973) for a listing of all the components.

TABLE 3
COLUMN DENSITIES TOWARD SN 1987A

ION	$\lambda(\text{\AA})$	Interval 1 ($v < 120 \text{ km s}^{-1}$)			Interval 2 ($120 < v < 190 \text{ km s}^{-1}$)			Interval 3 ($v > 190 \text{ km s}^{-1}$)		
		log N			log N			log N		
		l.l.	best ^a	u.l.	l.l.	best ^a	u.l.	l.l.	best ^a	u.l.
Al III	1854.72	13.09	13.12	13.15	11.49	11.64	11.73	13.45	13.49	13.53
Al III	1862.79	13.11	13.15	13.18	12.01	12.08	12.15	13.48	13.51	13.54
Si IV	1393.76	13.54	13.58	13.62	12.72	12.77	12.82	14.02
Si IV	1402.77	13.48	13.52	13.57	12.72	12.78	12.84	14.19
C IV	1548.20	14.10	14.15	14.21	13.36	13.41	13.46	14.59
C IV	1550.77	14.10	14.15	14.20	13.40	13.46	13.51	14.81

^a Lower limits (l.l.), best values, and upper limits (u.l.) to column densities for each high ionization absorption line are listed for the three indicated velocity ranges. These estimates are based on a direct integration of the optical depth profiles shown in Figures 2, 3 and 4. For the highest velocity range ($v > 190 \text{ km s}^{-1}$), we only list lower limits for the Si IV and C IV column densities. Near $v \approx 270$ to 280 km s^{-1} the Si IV and C IV optical depths are so large they can not be reliably measured (see §IIIb).

TABLE 4
COLUMN DENSITIES FOR HIGHLY IONIZED MILKY WAY HALO GAS

Ion	Predicted ^a N sin b	Halo Stars ^b < N sin b >	HD 5980 ^c N sin b	HD 36402 ^d N sin b	SN 1987A ^e N sin b
Al III	4.5x10 ¹²	4.6x10 ¹²	7.3x10 ¹²
Si IV	(3.3-6.4)x10 ¹²	≈2x10 ¹³	2.8x10 ¹³	1.8x10 ¹³	1.9x10 ¹³
C IV	(4.3-7.9)x10 ¹³	≈1x10 ¹⁴	1.8x10 ¹⁴	5.4x10 ¹³	7.7x10 ¹³
N V	(2.8-3.6)x10 ¹³	≈3x10 ¹³	2.2x10 ¹³	< 1.8x10 ¹³	...
O VI	(5.8-6.0)x10 ¹⁴	>3x10 ¹³

^a Predicted column densities of highly ionized gas through the halo (N Sin |b|) on one side of the galaxy based on the time-dependent ionization calculations of Edgar and Chevalier (1986). The values assume a fountain mass flow rate of 4M_☉/yr on each side of the galactic plane. The mass flow rate has been adjusted to provide approximate agreement for the average observed strength of N V absorption toward high |z| halo stars. The two values of column density listed for each ion involve different assumptions about the sizes of the cooling regions. These same calculations are able to explain the C IV and O III] emission measurements of Martin and Bowyer(1987) provided the fountain mass flow rate is about 2x larger than assumed above.

^b Observations are from Savage and Massa (1987) for Si IV, C IV and N V and from Jenkins (1978) for O VI. The value for O VI is listed as a lower limit because the measures only extend to |z| ≈ 1 kpc.

^c The values listed are for the sight line to HD 5980 in the SMC from Fitzpatrick and Savage (1983) and refer to gas with v < 100 km s⁻¹.

^d The values listed are for the sight line to HD 36402 in the LMC from Savage and de Boer (1981) and refer to gas with v < 120 km s⁻¹.

^e The listed column densities are for gas in the direction of SN 1987A with v < 120 km s⁻¹ (see Table 3).

TABLE 5

EXPECTED COLUMN DENSITIES OF Si II* (cm⁻²)

$\dot{M} / v_w [M_{\odot} \text{ yr}^{-1} (\text{km s}^{-1})^{-1}]$					
$5 \times 10^{-8} (\xi = 2)$	$5 \times 10^{-7} (\xi = 2)$	$1 \times 10^{-6} (\xi = 1)$	$1 \times 10^{-6} (\xi = 2)$	$2 \times 10^{-6} (\xi = 1)$	$2 \times 10^{-6} (\xi = 2)$
4.9×10^{10}	1.7×10^{12}	5.6×10^{12}	7.8×10^{12}	3.0×10^{13}	3.7×10^{13}

FIGURE CAPTIONS

Fig. 1.- Averaged high-resolution interstellar line profiles for SN 1987A based on the IUE spectra listed in Table 1. In most cases, four spectra have been averaged to produce the profiles shown. IUE flux has been plotted against heliocentric velocity for the lines listed in Table 2. The zero level of flux is indicated by the tic marks on the vertical axis. In some cases more than one ion absorbs in the spectral region illustrated (see the comments to Table 2). R indicates a detector reseau.

Fig. 2.- Plots of apparent $\log N(v)$ vs heliocentric velocity for three absorption lines of Si II: (1), $\lambda 1526.72$ with $\log f\lambda = 2.545$ (solid circles), (2) $\lambda 1304.37$ with $\log f\lambda = 2.283$ (solid squares), and (3) $\lambda 1808.00$ with $\log f\lambda = 2.545$ (open circles). $N(v)$ was defined according to Eqns. 1 and 2, and is clearly not valid for the two stronger lines, as explained in the text. Logarithms of the apparent optical depths τ for the three lines are indicated by the scales on the right-hand side. Small symbols above and below the main ones indicate the range of possible systematic errors caused by uncertainties in both the adopted continua and zero-intensity baselines (they *do not* show errors attributable to each point's uncertainty caused by noise).

Fig. 3.- Logarithmic plot of apparent optical depth τ (as defined by eq. 1) vs heliocentric velocity for the Al III 1854.72 Å line (solid circles) and 1862.80 Å line (open circles). The points for the 1862 Å line have been moved upward by 0.3 to correct for the fact that its transition probability is smaller by a factor of 2. As with Fig. 2, small symbols on either side of the main points indicate the range of *systematic* uncertainties. $\log \tau = 0$ on this diagram corresponds to $N(v) = 10^{11.58} \text{ cm}^{-2} (\text{km s}^{-1})^{-1}$ (see Eq. 2).

Fig. 4.- Logarithmic plot of apparent optical depth τ (as defined by eq. 1) vs heliocentric velocity for the Si IV 1393.76 Å line (solid circles) and 1862.80 Å line (open circles). The points for the 1402 Å line have been moved upward by 0.3 to correct for the fact that its transition probability is smaller by a factor of 2. As with Fig. 2, small symbols on either side of the main points indicate the range of *systematic* uncertainties. $\log \tau = 0$ on this diagram corresponds to $N(v) = 10^{11.71} \text{ cm}^{-2} (\text{km s}^{-1})^{-1}$ (see Eq. 2).

Fig. 5.- Logarithmic plot of apparent optical depth τ (as defined by eq. 1) vs heliocentric velocity for the C IV 1548.20 Å line (solid circles) and 1550.77 Å line (open circles). The points for the 1550 Å line have been moved upward by 0.3 to correct for the fact that its transition probability is smaller by a factor of 2. As with Fig. 2, small symbols on either side of the main points indicate the range of *systematic* uncertainties. Log $\tau = 0$ on this diagram corresponds to $N(v) = 10^{12.10} \text{ cm}^{-2} (\text{km s}^{-1})^{-1}$ (see Eq. 2).

Fig. 6.- $\log N(\text{Si IV}) - \log N(\text{Al III})$ versus heliocentric velocity derived from the apparent optical depth plots of Figures 4 and 3. Results are not plotted for those ranges of velocity where the apparent optical depths are unreliable. Si IV and Al III have very different line profiles which implies that their column density ratios change substantially with velocity as indicated in this figure.

Fig. 7.- $\log N(\text{C IV}) - \log N(\text{Al III})$ versus heliocentric velocity derived from the apparent optical depth plots of Figures 5 and 3. Results are not plotted for those ranges of velocity where the apparent optical depths are unreliable. C IV and Al III have very different line profiles which implies that their column density ratios change substantially with velocity as indicated in this figure.

Fig. 8.- $\log N(\text{C IV}) - \log N(\text{Si IV})$ versus heliocentric velocity derived from the apparent optical depth plots of Figures 5 and 4. Results are not plotted for those ranges of velocity where the apparent optical depths are unreliable. C IV and Si IV have similar line profiles which implies that their column density ratios are relatively independent of velocity.

Fig. 9.- Al III, Si IV, C IV Profiles for R136a, R 144, and HD 36402 from Savage and Meade (1989). Intensity is plotted versus heliocentric velocity with the zero level of intensity indicated by the tic marks on the vertical axis. R136a and R 144 are situated in the 30 Doradus nebula while HD 36402 lies beyond the boundaries of the nebula in its own H II region. The lines of Al III, Si IV and C IV toward SN 1987A (see Fig. 1a) are intermediate in strength between what is seen toward R136a and R 144. The complex pattern of motions of the nebular gas in the 30 Doradus region and beyond probably explains the differences in velocity of the high ionization absorption from one sight line to another. When looking directly toward the center of the nebula (e.g. toward R136a) the outflow velocities are rather extreme and produce nebular absorption features which overlap the absorption near zero velocity due to the Milky Way. R indicates a detector reseau and B indicates a bright pixel, most likely produced by a cosmic ray event. Each profile plotted represents an average of five spectra (for R136a and HD36402) or two spectra (for R144).

Fig. 10.- Hydrogen α $\lambda 6562.808$ emission line spectrum for a direction 10" south of SN 1987A. Intensity is plotted versus heliocentric velocity in km s^{-1} . Weak telluric $\text{H}\alpha$ is apparent along with the strong $\text{H}\alpha$ emission produced by H II region gas in the general vicinity of the supernova. The continuum is probably light from the supernova scattered into the spectrograph. This spectrum was obtained with the echelle spectrograph on CTIO 4 m telescope by Y. H. Chu (private communication).

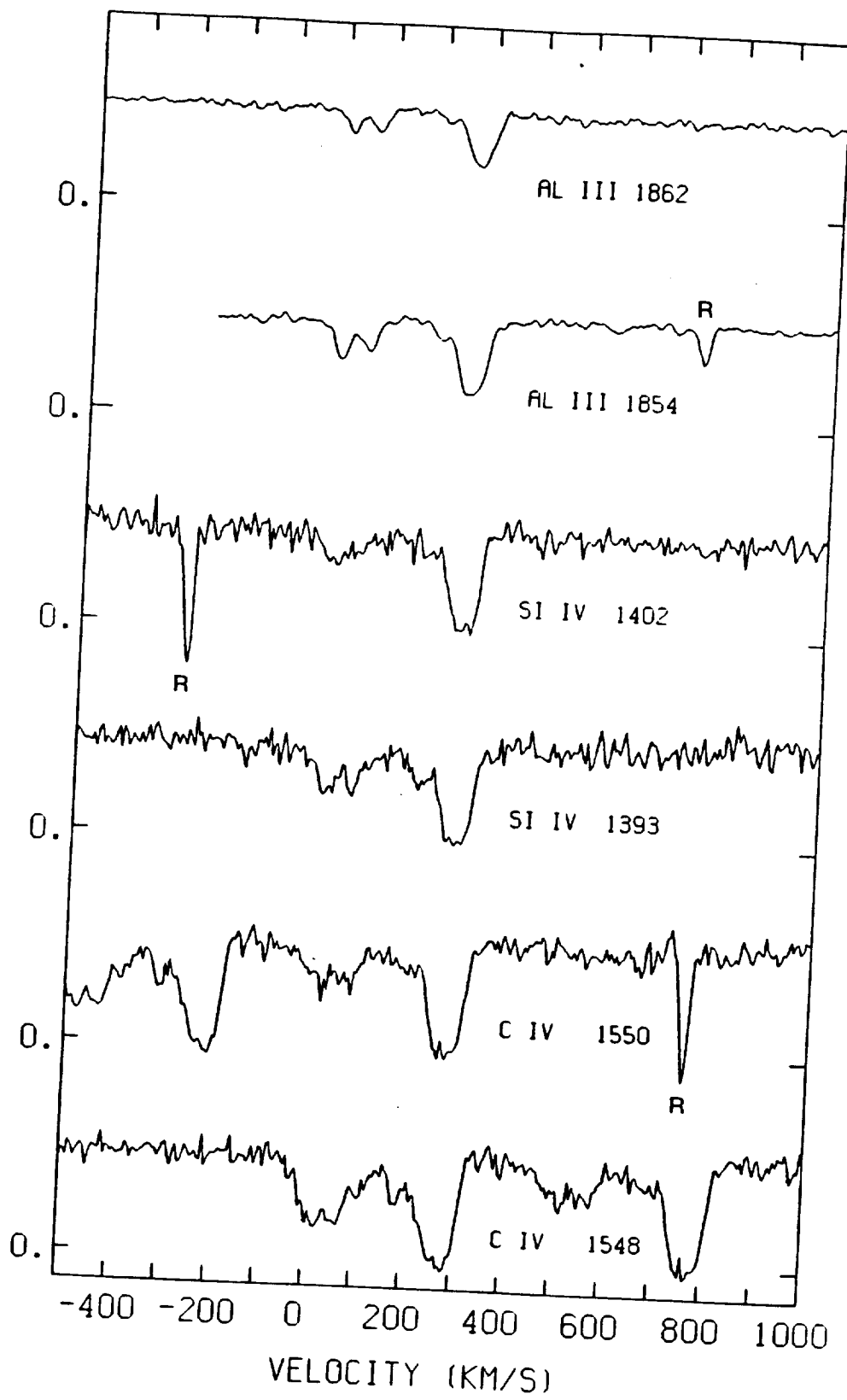


FIG. 1a

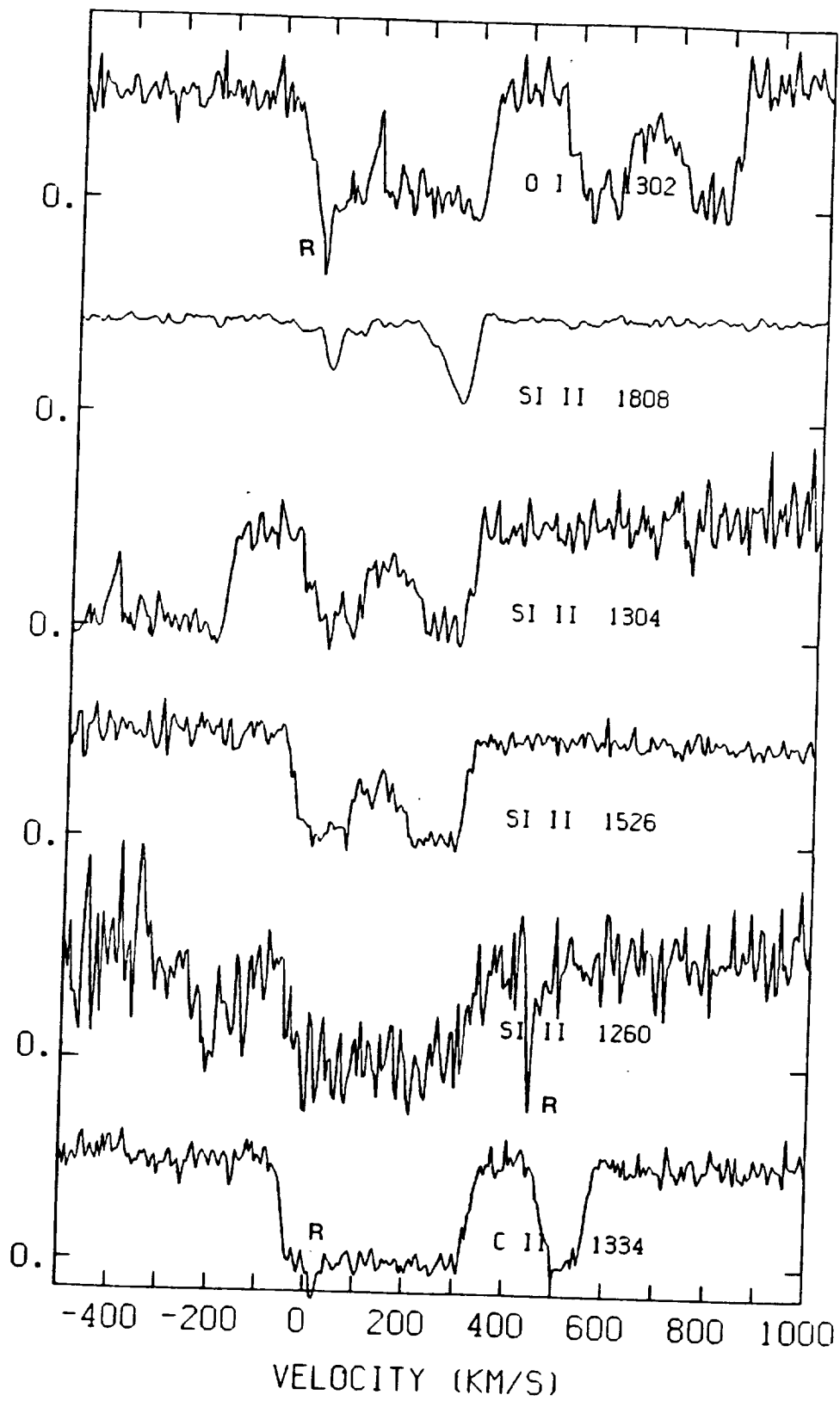


FIG. 1b

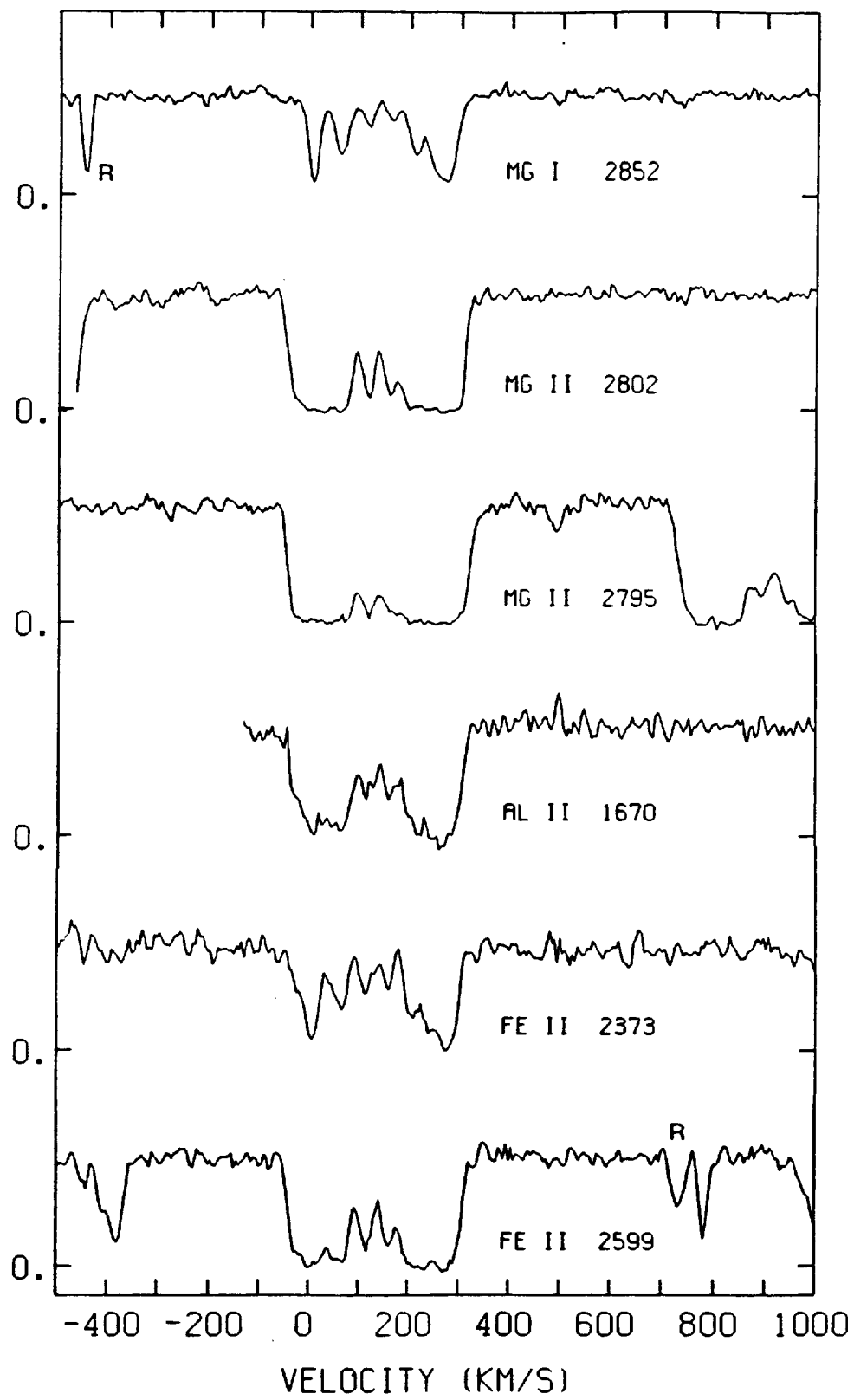


FIG. 1c

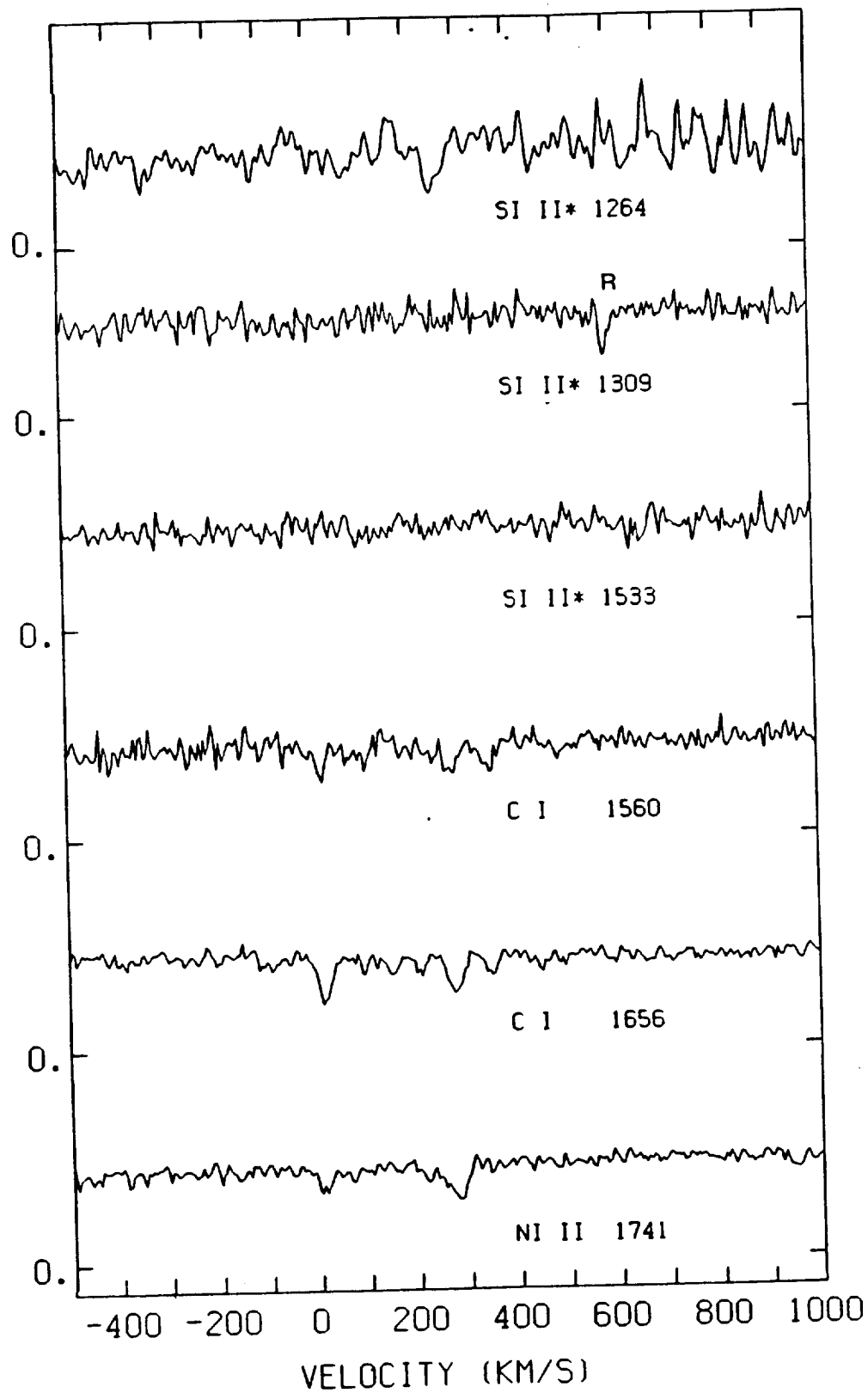


FIG. 1d

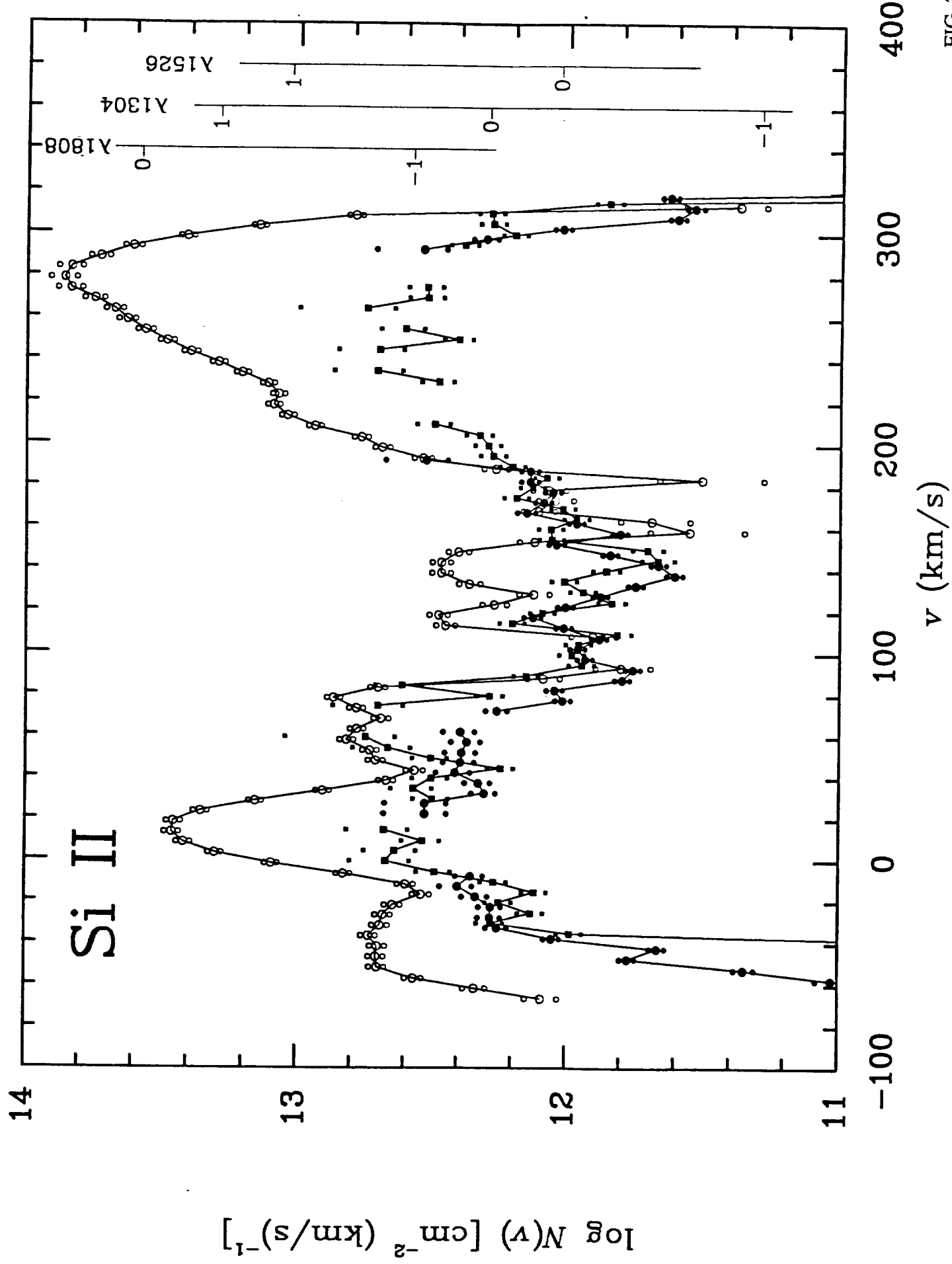


FIG. 2

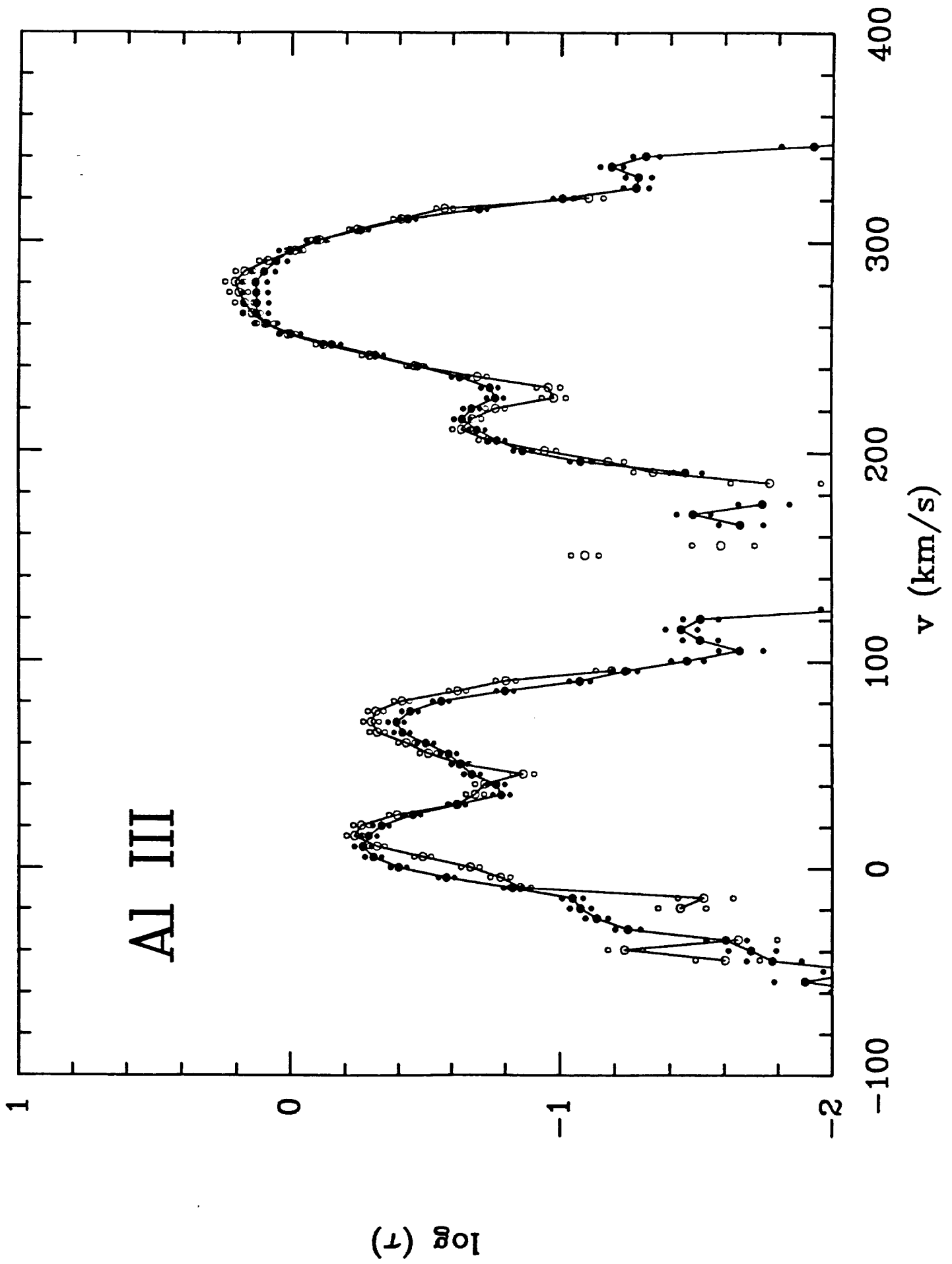


FIG. 3

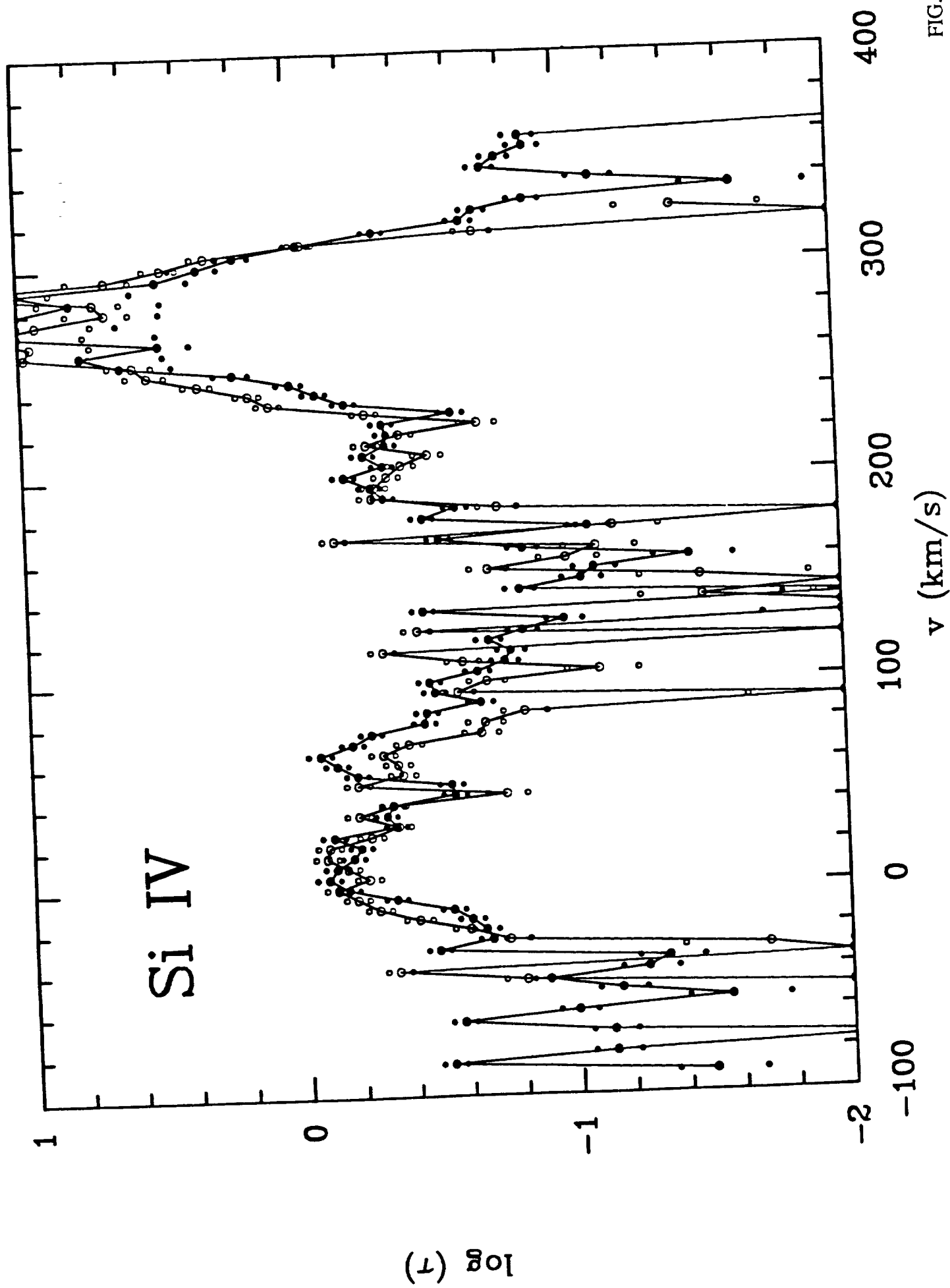


FIG. 4

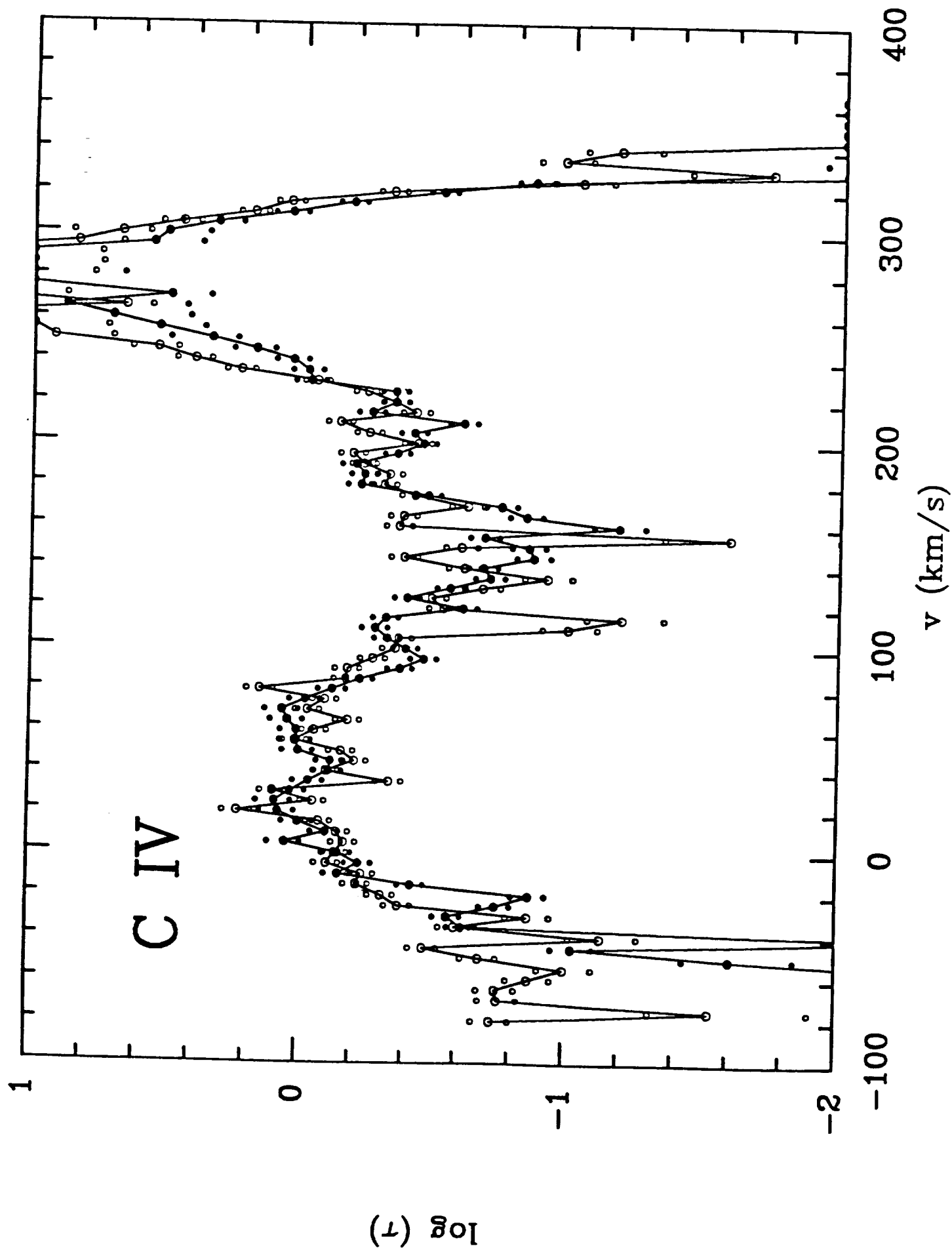


FIG. 5

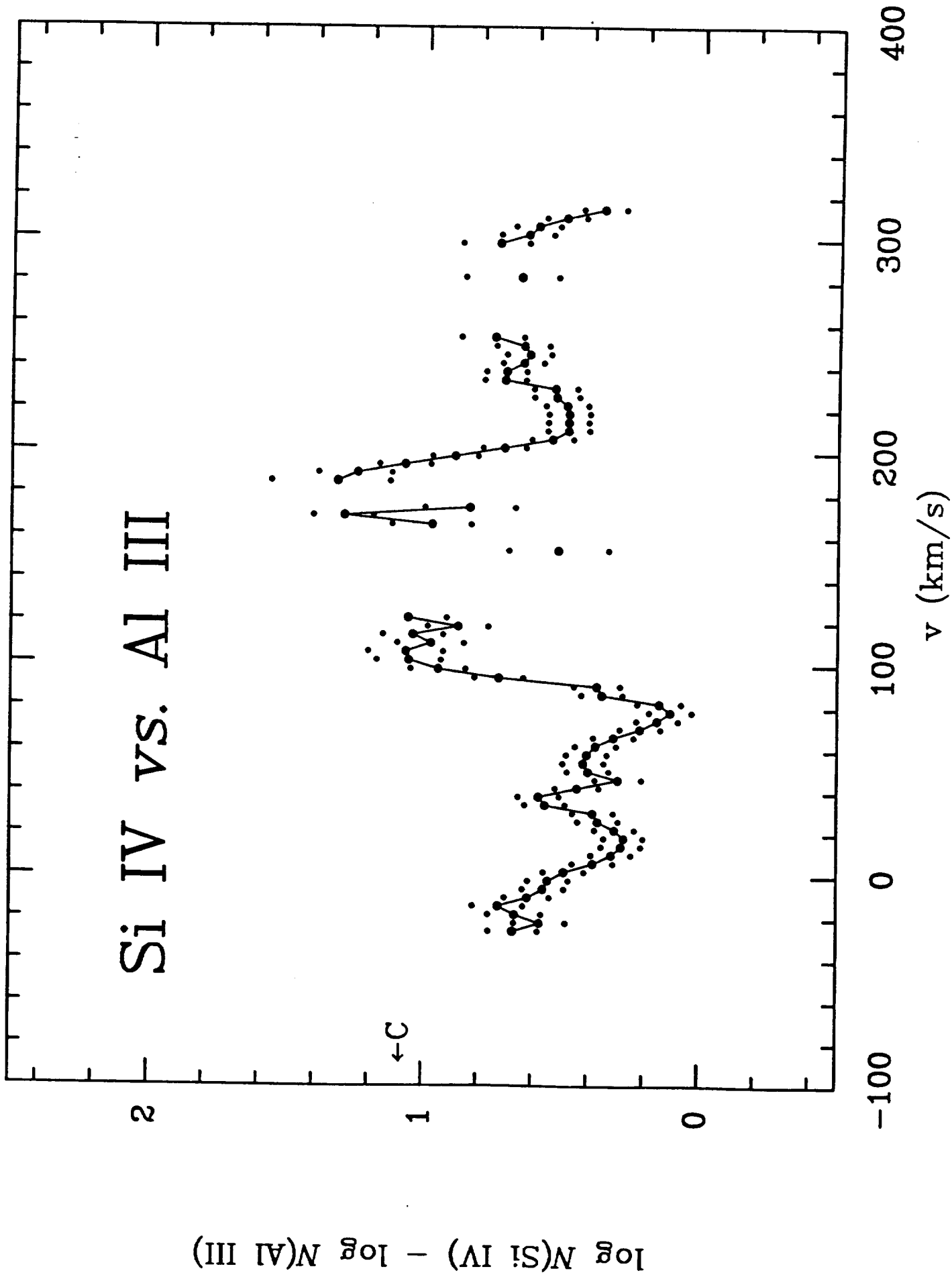


FIG. 6

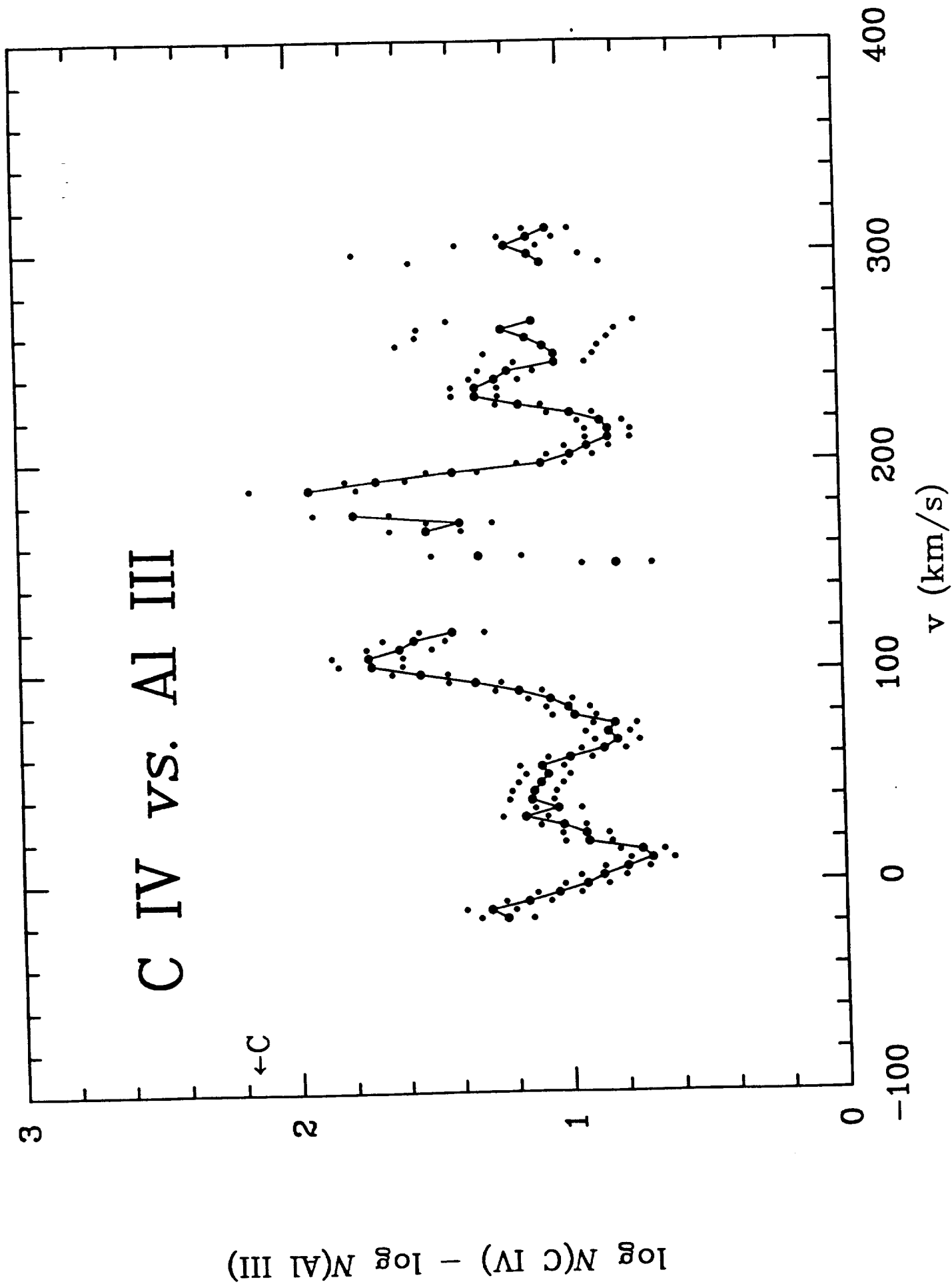


FIG. 7

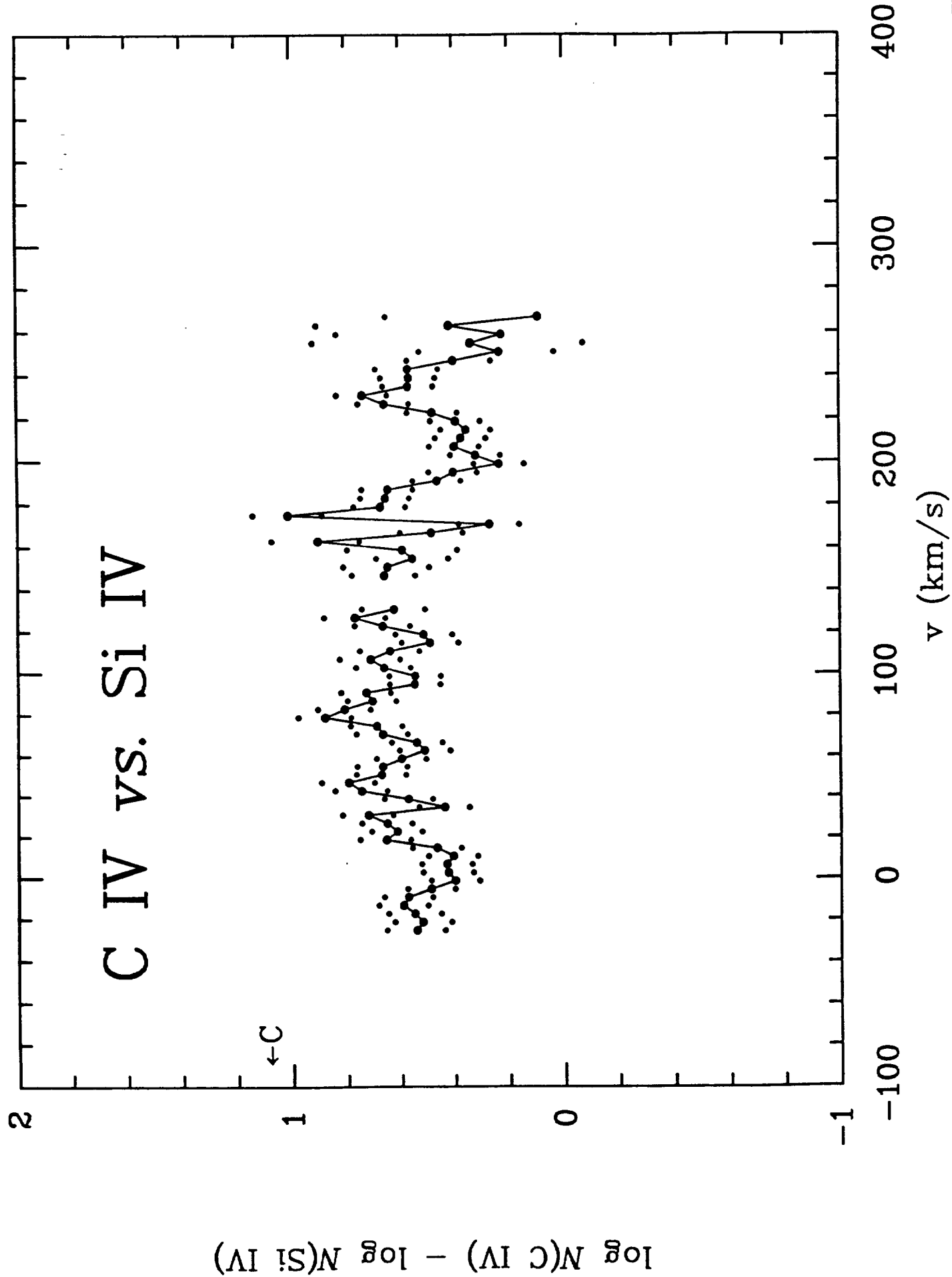


FIG. 8

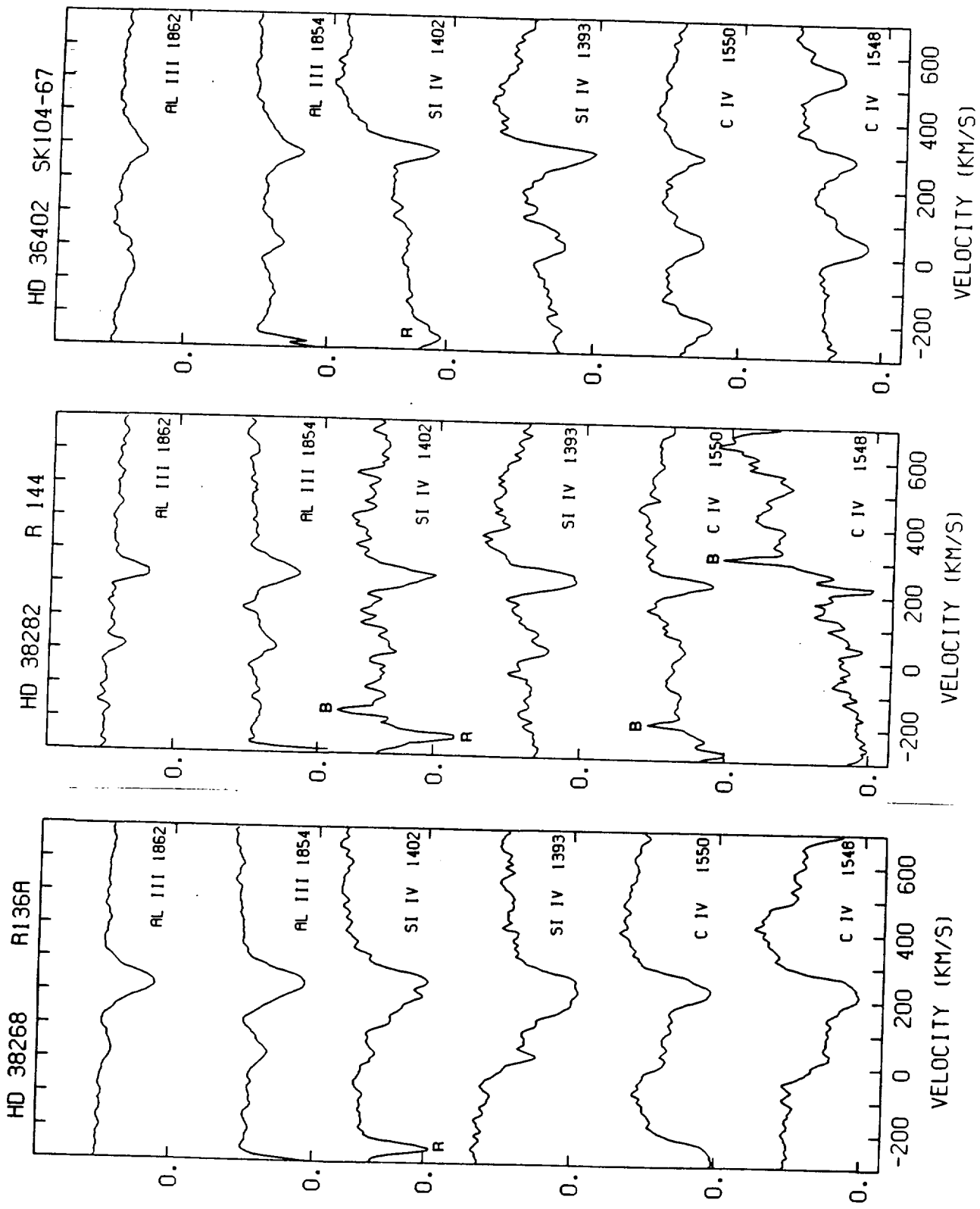


FIG. 9

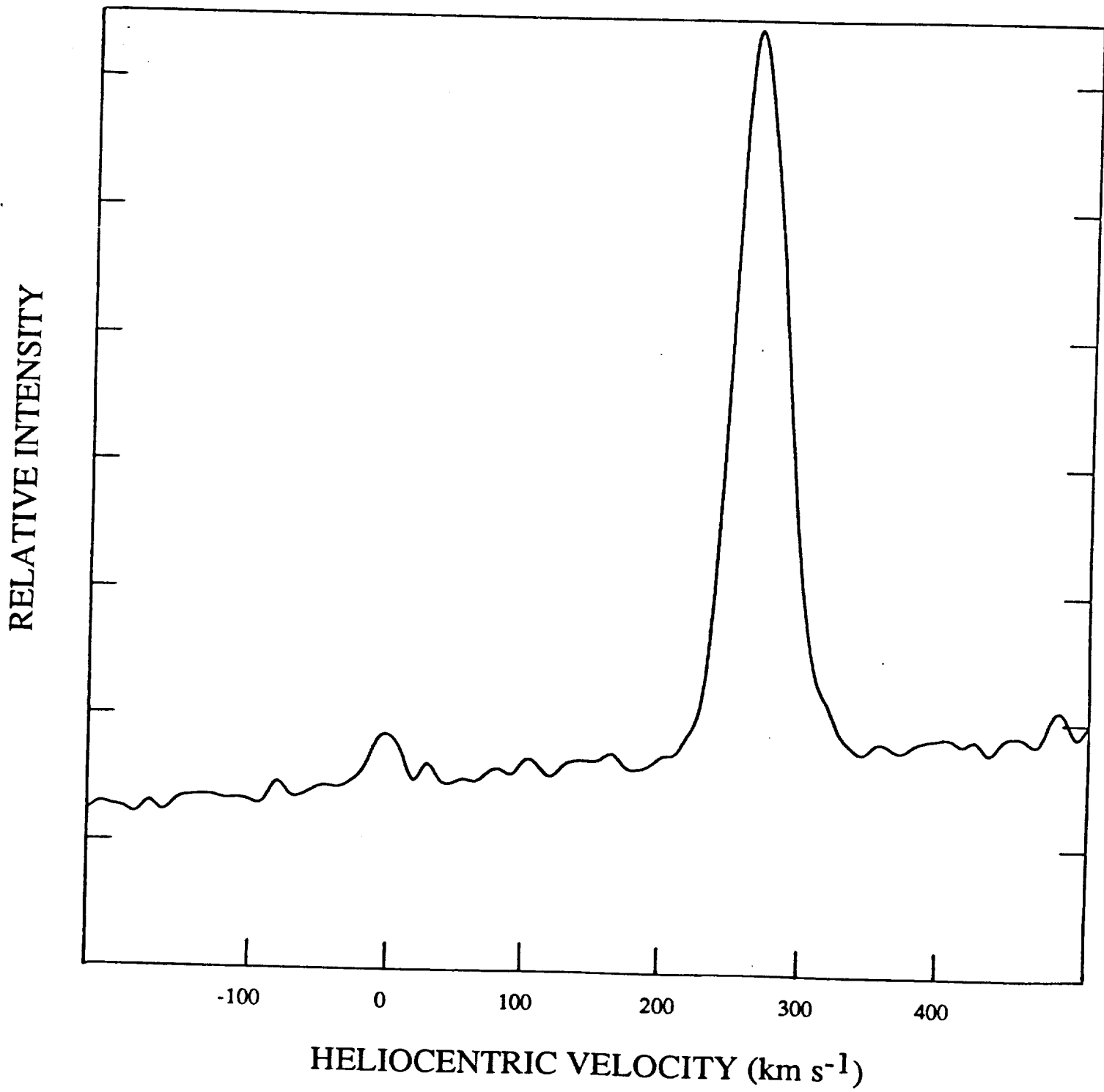


FIG. 10